The −603T > C variation is important on theoretical grounds, because a predictive analysis of binding motifs for transcription factors using the MatInspector program v2.2[16] revealed that the sequence surrounding this polymorphic site is sufficiently similar to the consensus binding sequence for a transcription factor, Nkx-2.5 (CAAAGTG, where the underlined A is a variant nucleotide). This putative binding site on the promoter of LIFR was intact on chromosomes carrying the −603T allele, but absent in homozygous carriers of C alleles. Although the functions of human Nkx-2.5 in bone tissues are not yet defined, LIFR might be one of its transcriptional targets.[17] Functional studies on this promoter region are ongoing in our laboratory, however, because physiological roles of single *cis*-element or *trans*-factor could not easily be determined by a simple assay, those studies would be presented in a future independent report. There also exists the possibility that the −603 polymorphism could be in linkage disequilibrium with unknown but functional variants nearby.

In summary, we showed a significant association between the −603T > C variation in the promoter region of the LIFR gene and radial BMD among adult Japanese women. Structural inspection proposed a possible contribution of a transcription factor, Nkx-2.5, that might bind to this SNP site. Functional biological studies as well as longitudinal studies may clarify the true mechanism of the association reported here.

Acknowledgments

This work was supported in part by a special grant for Strategic Advanced Research on 'Cancer' and 'Genome Science' from the Ministry of Education, Science, Sports and Culture of Japan; by a Research Grant for Research from the Ministry of Health and Welfare of Japan; and by a Research for the Future Program Grant of The Japan Society for the Promotion of Science.

References

1 Carol BW, Mark CH, Blair RR, Joan SH, Denny L. Targeted disruption of the low-affinity leukemia inhibitory factor receptor gene causes placental, skeletal, neural and metabolic defects and results in perinatal death. *Development* 1995; **121**: 1283–1299.
2 Orimo H, Hayashi Y, Fukunaga M *et al.* Diagnostic criteria for primary osteoporosis: year 2000 revision. *J Bone Miner Metab* 2001; **19**: 331–337.
3 Giguere Y, Rousseau F. The genetics of osteoporosis: 'complexities and difficulties'. *Clin Genet* 2000; **57**: 161–169.
4 Riggs BL, Melton LJ 3rd. Involutional osteoporosis. *N Engl J Med* 1986; **314**: 1676–1686.
5 Boyle WJ, Simonet WS, Lacey DL. Osteoclast differentiation and activation. *Nature* 2003; **423**: 337–342.
6 Jilka RL. Biology of the basic multicellular unit and the pathophysiology of osteoporosis. *Med Pediatr Oncol* 2003; **41**: 182–185.
7 Manolagas SC, Jilka RL. Bone marrow, cytokines, and bone remodeling. Emerging insights into the pathophysiology of osteoporosis. *N Engl J Med* 1995; **332**: 305–311.
8 Pfeilschifter J, Koditz R, Pfohl M, Schatz H. Changes in proinflamatory cytokine activity after menopause. *Endocrine Rev* 2002; **23**: 90–119.
9 Heinrich PC, Behermann I, Haan S, Hermanns HM, Muller NG, Schaper F. Principles of interleukin (IL)-6-type cytokine signalling and its regulation. *Biochem J* 2003; **374**: 1–20.
10 Ishida R, Ezura Y, Iwasaki H *et al.* Linkage disequilibrium and haplotype analysis among four novel single-nucleotide polymorphisms in the human leukemia inhibitory factor (LIF) gene. *J Hum Genet* 2001; **46**: S57–559.
11 Metcalf D, Gearing DP. A myelosclerotic syndrome in mice engrafted with cells producing high levels of leukemia inhibitory factor (LIF). *Leukemia* 1989; **3**: 847–852.
12 Dagoneau N, Scheffer D, Huber C *et al.* Null leukemia inhibitory factor receptor (LIFR) mutations in Stuve-Wiedemann/Schwartz–Jampel type 2 syndrome. *Am J Hum Genet* 2004; **74**: 298–305.
13 Iwasaki H, Emi M, Ezura Y *et al.* Association of a Trp16Ser variation in the gonadotropin releasing hormone signal peptide with bone mineral density, revealed by SNP-dependent PCR typing. *Bone* 2003; **32**: 185–190.
14 Kleinbaum DG, Kupper LL, Muller KE. *Applied Regression Analysis and Other Multivariate Methods*, 2nd edn. Boston: PWS-KENT Publishing, 1988; 299–301.
15 Stewart TL, Ralston SH. Role of genetic factors in the pathogenesis of osteoporosis. *J Endocrinol* 2000; **166**: 235–245.
16 Quandt K, Frech K, Karas H, Wingender E, Werner T. MatInd and MatInspector: new fast and versatile tools for detection of consensus matches in nucleotide sequence data. *Nucl Acids Res* 1995; **23**: 4878–4884.
17 Chen CY, Schwartz RJ. Identification of novel DNA binding targets and regulatory domains of a murine tinman homeodomain factor, nkx-2.5. *J Biol Chem* 1995; **270**: 15628–15633.

ELSEVIER

Molecular and Cellular Endocrinology 218 (2004) 147–153

MCE
Molecular and Cellular Endocrinology

www.elsevier.com/locate/mce

Systemic distribution of estrogen-responsive finger protein (Efp) in human tissues

Norihiro Shimada [a,b,*], Takashi Suzuki [a], Satoshi Inoue [c], Katsuaki Kato [b], Akira Imatani [b], Hitoshi Sekine [b], Syuichi Ohara [b], Tooru Shimosegawa [b], Hironobu Sasano [a]

[a] *Department of Pathology, Tohoku University School of Medicine, 2-1 Seiryo-machi, Aoba-ku, Sendai 980-8575, Japan*
[b] *Department of Gastroenterology, Tohoku University School of Medicine, Sendai, Japan*
[c] *Division of Gene Regulation and Signal Transduction, Research Center for Genomic Medicine, Saitama Medical School, Saitama, Japan*

Received 30 September 2003; accepted 3 December 2003

Abstract

Estrogen-responsive finger protein (Efp), a target gene product of estrogen receptor (ER), is considered essential for estrogen-dependent cell proliferation. The biological significance of Efp remains unclear in human tissues, and therefore, we examined systemic distribution of Efp in human adult and fetal tissues using RT-PCR and immunohistochemistry. Efp mRNA expression was marked in the placenta and uterus, high in the thyroid gland, aorta, and spleen in adult, and relatively low in other human adult and fetal tissues examined in this study. Efp immunoreactivity was detected in epithelium of various adult tissues, and was also detected in cytotrophoblasts of the placenta and splenic macrophages. Efp immunolocalization in human fetus was generally similar as that in adult. These Efp-positive cells were previously reported to be associated with ERα and/or ERβ expression. Therefore, these results indicate that Efp is widely expressed and may play important roles in various human tissues possibly through ERs.

Keywords: Distribution; Estrogen-responsive finger protein (Efp); Human tissues; Immunohistochemistry; Reverse transcriptase-polymerase chain reaction (RT-PCR)

1. Introduction

It is well known that estrogen plays important roles, not only in female reproductive organs but also in various tissues such as bone, liver, central nervous system (CNS) and cardiovascular system (Dickson and Stancel, 2000; Albertazzi and Purdie, 2001). Biological effects of estrogen are mediated through an interaction with the estrogen receptor (ER). Recently, a second ER, ERβ, has been identified in human (Kuiper et al., 1996; Mosselman et al., 1996), and the previously known human ER has been renamed ERα. ERβ is detected in various human tissues, including in both adult and fetus (Taylor and Al-Azzawi, 2000; Takeyama et al., 2001), while ERα is mainly expressed in female reproductive organs. ERs activate transcription by binding to estrogen-responsive elements (EREs) located in the promoter regions of target genes (Tsai and O'Malley, 1994). A variety of estrogenic functions are characterized by the expression of the estrogen-responsive genes following the binding of receptor protein to EREs (Inoue et al., 1993; Orimo et al., 1999).

Estrogen-responsive finger protein (Efp) belongs to a member of RING- finger B-box Coiled-Coil family (Inoue et al., 1993), which is considered to be involved in the regulation of various cellular functions, including cell-cycle regulation and transcription (Saurin et al., 1996). Efp has been isolated by genomic binding site cloning using a recombinant ER protein, and Efp gene has an ERE at the 3′-untranslated region (Inoue et al., 1993). Efp mRNA was also detected in MCF-7 human breast carcinoma cell line, and was rapidly induced by estrogen treatment within 0.5 h (Ikeda et al., 2000). Efp is mainly expressed in female reproductive organs and brain in mice (Orimo et al., 1995), and the study of Efp knockout mice revealed that Efp is essential for cell growth mediated by estrogen in the uterus (Orimo et al., 1999). In human, Efp expression has been reported

* Corresponding author. Tel.: +81-22-717-8050; fax: +81-22-717-8053.
E-mail address: nshimada@int3.med.tohoku.ac.jp (N. Shimada).

0303-7207/$ – see front matter © 2004 Elsevier Ireland Ltd. All rights reserved.
doi:10.1016/j.mce.2003.12.008

in breast tissues (Ikeda et al., 2000; Thomson et al., 2001; Urano et al., 2002), and Efp is postulated to be involved in the mammary gland differentiation (Thomson et al., 2001). However, Efp has not been examined in other human tissues, although estrogenic actions have been demonstrated in various human tissues, and the biological significance of Efp in relation to systemic estrogenic actions remains unclear. Therefore, in this study, we examined systemic distribution of Efp in human adult and fetal tissues using reverse transcription/real-time polymerase chain reaction (RT/real-time PCR) and immunohistochemistry.

2. Materials and methods

2.1. Tissue collection and preparation

Nonpathological human adult tissues ($n = 6$, respectively) were retrieved from autopsy files at Tohoku University Hospital (Sendai, Japan). Specimens of nonneoplastic area of human uterus ($n = 5$) were obtained from women who underwent hysterectomy for cervical carcinoma at the Department of Obstetrics and Gynecology, Tohoku University Hospital, and informed consent was obtained from these patients before the surgery. Human fetal tissues ($n = 5$, respectively) were obtained from fetuses aged 12–21 weeks gestation after elective termination in normal pregnant women at Nagaike Maternal Clinic (Sendai, Japan), and informed consent was obtained before the elective termination. The specimens were fixed in 10% formalin and embedded in paraffin wax. Histological examinations revealed no significant pathologic abnormalities in these tissues.

RT/real-time PCR analyses were also performed using snap-frozen samples stored at −80 °C. The type of tissues and the number of specimens examined in this study were listed in Table 2.

This study protocol was approved by the ethics committee of Tohoku University School of Medicine (Sendai, Japan).

2.2. RT/real-time PCR

Total RNAs were isolated using TRIzol regent (Life Technologies Inc., Grand Island, NY, USA), and used for the first-strand cDNA synthesis with Superscript II reverse transcriptase and oligo $(dT)_{12-18}$ primer (Life Technologies Inc., Gaitherburg, MD, USA). The forward and reverse primers for Efp mRNA were designed in the different exon to avoid the amplification of genomic DNA (Table 1). Oligonucleotide primers for glyceraldehyde-3-phosphate dehydrogenase (GAPDH) (Tokunaga et al., 1987) were also used as internal standard in this study.

The Light Cycler System (Roche Diagnositics GmbH, Mannheim, Germany) with FastStart DNA Master SYBER Green I (Roche Diagnostics GmbH) was used to obtain relative levels of Efp mRNA expression by real-time PCR (Dumoulin et al., 2000). An initial denaturing step of 95 °C for 10 min was followed by 40 cycles, respectively, of 95 °C for 15 s; 10 s annealing at 64 °C (Efp) or 60 °C (GAPDH); and extension for 10 s at 72 °C. The fluorescence intensity of the double-strand specific SYBER Green I, which reflects the amount of formed specific PCR products, was read by the Light Cycler at 86 °C after the end of each extension step. After PCR, these products were resolved on a 2% agarose ethidium bromide gel. PCR products were purified and subjected to direct sequencing (ABI PRISM BigDye Terminator Cycle Sequencing Ready Reaction Kit and ABI PRISM 310 Genetic Analyzer, Perkin-Elmer Corp., PE Applied Biosystems, Foster City, CA, USA) to verify amplification of the correct sequences.

As positive controls, breast cancer cell line MCF-7 was used (Ikeda et al., 2000). Negative control experiments lacked cDNA substrate to check for the possibility of exogenous contaminant DNA, and no amplified products were detected. The mRNA levels of Efp were adjusted to the levels of GAPDH and expressed as the ratio per those in MCF-7 (100%).

2.3. Immunohistochemistry

Immunohistochemical analysis was performed by employing the streptavidin–biotin amplification method using a Histofine Kit (Nichirei, Tokyo, Japan). The dilution of human Efp monoclonal antibody (Inoue et al., 1993) was 1/5000 in this study. The antigen-antibody complex was visualized with 3,3′-diaminobenzidine (DAB) solution (1 mM DAB, 50 mM Tris–HCl buffer (pH 7.6), and 0.006% H_2O_2), and counterstained with methyl green or hematoxylin. Human breast tissues were used as positive control for Efp immunostaining (Ikeda et al., 2000; Thomson et al., 2001). For negative controls, normal mouse IgG instead of the primary antibody was used, and no specific immunoreactivity was detected in these sections. To identify Efp positive cells in the spleen, we also performed immunohistochemistry for CD68 (DAKO, Carpinteria, CA, USA) using the serial sections.

Table 1
Primer sequences utilized in RT/real-time PCR analysis

cDNA		Primer sequences (5′–3′)	cDNA position	Size (bp)
Efp (D21205)	Forward	AACATCTCTCAAGGCCAAGGT	1338–1358	287
	Reverse	AGATGCCTACCCCACAGAAGT	1604–1624	
GAPDH (M33197)	Forward	TGAACGGGAAGCTCACTGG	731–750	307
	Reverse	TCCACCACCCTGTTGCTGTA	1018–1038	

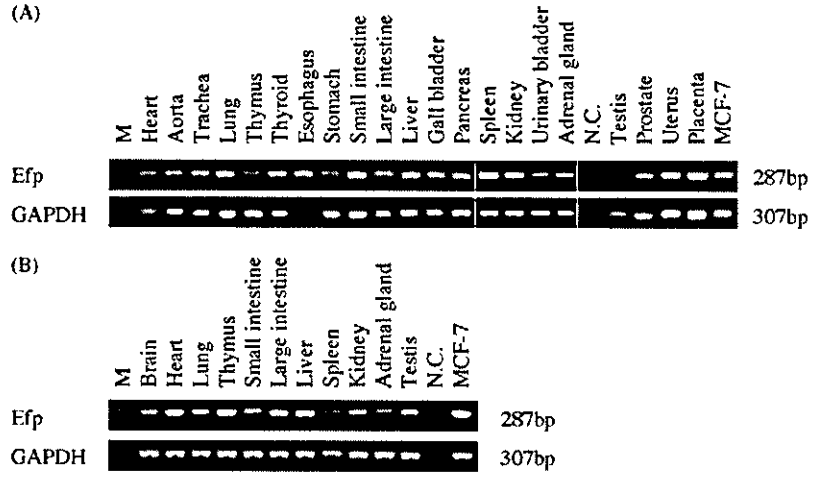

Fig. 1. Reverse transcription/real-time polymerase chain reaction (RT/real-time PCR) analysis for Efp in various human tissues in adult (A) and fetus (B). mRNA expression for Efp was detected as a specific single band (287 bp) in various human tissues both in adult (A) and fetus (B) (upper panels, respectively). Efp mRNA was not detected in adipose tissue in adult. In this study, mRNA expression for glyceraldehyde-3-phosphate dehydrogenase (GAPDH) was also detected as a specific single band (307 bp) in each specimen examined (lower panels, respectively). NC: negative control (no cDNA substrate); MCF-7: positive control. Representative samples were shown in this agarose gel photo.

3. Results

3.1. RT/real-time PCR

As shown in Fig. 1A and B, mRNA expression for Efp and GAPDH was detected as a specific single band (287 bp for EFP and 307 bp for GAPDH) by RT/real-time PCR analysis. Results of Efp mRNA expression levels in various human tissues were summarized in Table 2. Efp mRNA expression was abundantly detected in the placenta (159.2%) and uterus (95.7%). Efp mRNA expression was also high in the thyroid gland, aorta, and spleen in adult (12.5–12.8%). Efp mRNA expression was relatively low in other human adult and fetal tissues examined (≦10.5%).

3.2. Immunohistochemistry

Results of immunohistochemistry for Efp were summarized in Table 3. In adult, Efp immunoreactivity was detected in the cytoplasm of epithelium in various tissues (Fig. 2A–F). In some glandular epithelia, Efp immunoreactivity was tended to be marked at the luminal side (Fig. 2F). In addition, Efp immunoreactivity was detected in the cytotrophoblasts, but not syncytiotrophoblasts (Fig. 2G) of the placenta and vascular endothelium. Efp immunoreactivity was also positive in CD68-positive splenic macrophages in the spleen (Fig. 2H and I).

Patterns of Efp immunolocalization in fetus were generally similar as these in adult (Fig. 2J–L), however, no significant immunoreactivity was detected in the fetal lung, and spleen in this study. Efp immunoreactivity was detected in chondrocytes of cartilage in fetus, whereas it was not significant in adult cartilage.

Table 2
Efp mRNA expression in human tissues

Tissues	Adult		Fetus	
	n	mRNA level (%)	*n*	mRNA level (%)
Placenta	4	159.2 ± 98.6	NA	
Uterus	5	95.7 ± 34.4	NA	
Testis	1	7.9	1	2.0
Prostate	3	4.9 ± 3.6	NA	
Thyroid gland	6	12.5 ± 7.5	NA	
Adrenal gland	5	3.5 ± 2.0	1	0.2
Brain	NA		1	1.4
Heart	4	7.1 ± 3.0	2	3.7 ± 0.9
Aorta	2	12.8 ± 7.9	NA	
Trachea	3	8.4 ± 4.2	NA	
Lung	5	5.3 ± 3.4	2	8.2 ± 3.8
Thymus	1	3.6	2	8.2 ± 3.1
Esophagus	3	1.1 ± 1.1	NA	
Stomach	4	0.5 ± 0.4	NA	
Small intestine	5	1.3 ± 0.8	1	0.8
Large intestine	5	3.1 ± 1.8	1	9.5
Liver	5	4.6 ± 3.1	3	5.9 ± 2.3
Gall bladder	3	2.0 ± 1.6	NA	
Pancreas	3	6.1 ± 3.4	NA	
Spleen	6	12.8 ± 7.6	1	0.1
Kidney	6	10.5 ± 5.9	2	1.2 ± 0.7
Urinary bladder	1	0.6	NA	

The mRNA level of Efp was summarized as a ratio of GAPDH and evaluated as a ratio (%) compared with that of positive control (MCF-7 cells = 100%). Data represent mean ± S.E.M. (more than two samples) or mean ± percent difference (two samples). NA: samples were not available.

4. Discussion

In this study, Efp mRNA was abundantly detected in the placenta (cytotrophoblasts) and uterus (endometrial glandular or epithelial cells). In the placenta, estrogen is gen-

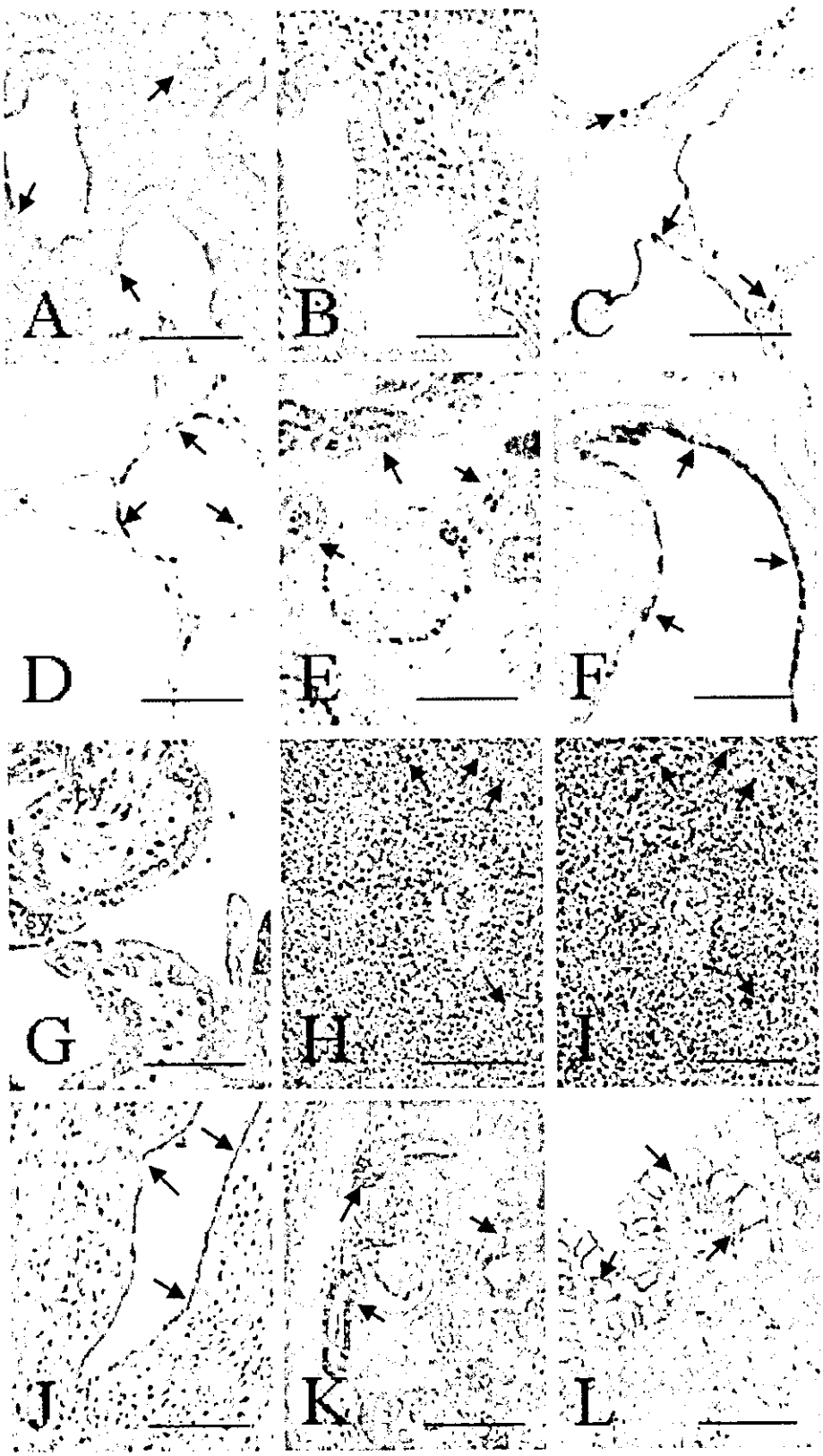
A
B
C
D
E
F
G
sy
sy
H
I
J
K
L

Table 3
Immunolocalization of Efp in human tissues

Tissues	Types of Efp positive cell			
	n	Adult	*n*	Fetal
Placenta	3	Cytotrophoblasts, decidual cell	0	NA
Uterus	3	Endometrial epithelial cell	2	Endometrial epithelial cell
Testis	3	Ductal cell, leydig cell	3	Ductal cell, mesenchymal cell
Prostate	2	Grandular epithelium	0	NA
Thyroid gland	3	Follicular epithelium	1	Follicular epithelium
Adrenal gland	5	None	2	None
Brain	0	NA	5	Nerve cell
Heart	2	None	2	None
Aorta and blood vessel	2	Endothelial cell	2	Endothelial cell
Trachea and bronchus	2	Epithelial cell	5	Epithelial cell
Lung	4	Alveolar epithelium	4	None
Thymus	2	Thymic epithelial cell	3	Thymic epithelial cell
Esophagus	2	Glandular epithelium	1	None
Stomach	2	None	3	None
Small and large intestine	3	Epithelial cell	4	Epithelial cell
Liver	2	Hepatocyte	3	Hepatocyte
Gall bladder	5	None	0	NA
Pancreas	2	Ductal epithelium	2	Ductal epithelium
Spleen	2	Splenic macrophage	2	None
Kidney	3	Epithelium of proximal tubule	2	Epithelium of proximal tubule
Urinary bladder	2	Transitional epithelium	3	Transitional epithelium
Cartilage	2	None	5	Chondrocyte
Salivary gland	2	Ductal epithelium	0	NA

NA: samples were not available; none: there was not significant immunoreactivity.

erally considered to play an important role in the regulation of placental function. ERα was expressed in cytotrophoblast cells, not in syncytiotrophoblast cells, and diminution of ERα and appearance of ERβ were demonstrated to be associated with the development of syncytiotrophoblast cells (Bukovsky et al., 2003a,b). Orimo et al. (1995) demonstrated that Efp was mainly expressed in female reproductive organs in mice, including uterus, ovary, and mammary gland, and was colocalized with ER. The study of Efp knockout mice subsequently revealed that Efp is essential for estrogen-induced cell proliferation as one of the direct targets of ERα (Orimo et al., 1999). Therefore, it is suggested that Efp is closely involved in the estrogenic actions, including the growth and/or differentiation, in these female reproductive organs through ERα.

High level of Efp mRNA expression was also detected in the aorta (endothelial cells) and spleen (splenic macrophages). Estrogen modulates vascular functions, and vascular endothelium is associated with expression of both ERα and ERβ (Suzuki et al., 2003). Estrogen reduces the vascular injury in wild-type, ERα knockout (ERαKO) (Sullivan et al., 1995; Iafrati et al., 1997), and ERβKO (Karas et al., 1999), but could not reduce the injury in ERαβ double KO mice (Karas et al., 2001). ERs were also detected in splenic macrophages (Kramer and Wray, 2002). Erlandsson et al. (2001) further demonstrated that deletion of ERα led to hypoplasia of spleen in their study using ERαKO, ERβKO, and ERαβ double KO mice. However the detailed estrogenic functions remain unclear in human aorta or spleen. Therefore the estrogenic actions in these tissues above may be partly through the Efp expression.

In our study, relatively low levels of Efp mRNA expression were detected in various tissues including those in which the expression of ERs has been reported. Among human tissues examined, Efp immunoreactivity was mainly detected in the epithelial cells. Previous studies demonstrated the widespread distribution of ERβ in various human tissues both in adult and fetus (Taylor and Al-Azzawi, 2000; Takeyama et al., 2001). ERβ immunoreactivity was strongly detected in the follicular epithelium of human thyroid gland

Fig. 2. Immunohistochemistry for Efp in human tissues. Efp immunoreactivity was detected in the endometrial epithelial cells in the uterus (A). No immunoreactivity was detected in the negative control using the serial section (B). In the lung, Efp immunoreactivity was detected in the alveolar epithelium (arrows) (C). Efp immunoreactivity was detected in follicular epithelium of the thyroid gland (arrows) (D). In the kidney, Efp immunoreactivity was detected in epithelium of the proximal tubule (arrows) (E). Glandular epithelial cells (arrows) were positive for Efp in the esophagus (F). In the placenta, Efp was positive in the cytotrophoblast (cy) but not syncytiotrophoblasts (sy) (G). In the spleen, Efp immunoreactivity was sporadically found in the marginal zone (H). These cells were also positive for CD68 (arrows) in the serial section (I), suggesting the splenic macrophages. Hematoxylin was used for counterstaining in (I). In fetal aorta, Efp immunoreactivity was detected in endothelial cells (arrows) (J). Efp immunoreactivity was detected in epithelium of the proximal tubule (arrows) in the fetal kidney (K). Efp was immunolocalized in the epithelium of the fetal colon (L): bar = 100 μm, respectively.

from 11 gestational weeks, suggesting the important estrogen actions in the development and/or maintenance of thyroid follicular functions through ERβ (Kawabata et al., 2003). ERβ was also reported in glandular epithelium of the prostate (Tsurusaki et al., 2003), epithelium of respiratory system (Taylor and Al-Azzawi, 2000), and epithelium of the stomach (Matsuyama et al., 2002) and colon (Konstantinopoulos et al., 2003), where Efp immunoreactivity was detected in our present immunohistochemical study. On the other hand, ERβ was also detected in interstitial cells such as adipocytes, smooth muscle cells and fibroblasts (Taylor and Al-Azzawi, 2000; Joyner et al., 2001; Haczynski et al., 2002), while Efp immunoreactivity was not detected in these cells in our present study. Therefore, Efp is considered to be involved in the regulation of estrogen related functions in epithelial cells in these tissues, possibly through ERβ, but not in that of stromal cells.

In summary, our present results demonstrated that Efp is widely expressed in human adult and fetal tissues. The Efp-positive cells were generally associated with the expression of ERα and/or ERβ previously, and therefore, it is suggested that Efp plays important roles in various human tissues possibly through ERs. Further examinations, including functional studies, are required to clarify these hypotheses or to understand the detailed biological significance of Efp in human tissues.

Acknowledgements

We thank Dr. F. Nagaike (Nagaike Maternal Clinic) and Dr. K. Kitamura (Department of Obstetrics and Gynecology, Tohoku University Hospital) for providing tissue samples. We appreciate the skillful technical assistance of Ms. Y. Murakami, Ms. C. Kaneko and Mr. K. Ono in the Department of Pathology, Tohoku University School of Medicine.

References

Albertazzi, P., Purdie, D.W., 2001. The life and times of the estrogen receptors: an interim report. Climacteric 4, 194–202.

Bukovsky, A., Cekanova, M., Caudle, M.R., Wimalasena, J., Foster, J.S., Henley, D.C., Elder, R.F., 2003a. Expression and localization of estrogen receptor-alpha protein in normal and abnormal term placentae and stimulation of trophoblast differentiation by estradiol. Reprod. Biol. Endocrinol. 1, 13.

Bukovsky, A., Caudle, M.R., Cekanova, M., Fernando, R.I., Wimalasena, J., Foster, J.S., Henley, D.C., Elder, R.F., 2003b. Placental expression of estrogen receptor beta and its hormone binding variant—comparison with estrogen receptor alpha and a role for estrogen receptors in asymmetric division and differentiation of estrogen-dependent cells. Reprod. Biol. Endocrinol. 1, 36.

Dickson, R.B., Stancel, G.M., 2000. Estrogen receptor-mediated processes in normal and cancer cells. J. Natl. Cancer Inst. Monogr. 27, 135–145.

Dumoulin, F.L., Nischalke, H.D., Leifeld, L., von dem Bussche, A., Rockstroh, J.K., Sauerbruch, T., Spengler, U., 2000. Semi-quantification of human C–C chemokine mRNAs with reverse transcription/real-time PCR using multi-specific standards. J. Immunol. Methods 241, 109–119.

Erlandsson, M.C., Ohlsson, C., Gustafsson, J.A., Carlsten, H., 2001. Role of oestrogen receptors alpha and beta in immune organ development and in oestrogen-mediated effects on thymus. Immunology 103, 17–25.

Haczynski, J., Tarkowski, R., Jarzabek, K., Slomczynska, M., Wolczynski, S., Magoffin, D.A., Jakowicki, J.A., Jakimiuk, A.J., 2002. Human cultured skin fibroblasts express estrogen receptor alpha and beta. Int. J. Mol. Med. 10, 149–153.

Iafrati, M.D., Karas, R.H., Aronovitz, M., Kim, S., Sullivan Jr., T.R., Lubahn, D.B., O'Donnell Jr., T.F., Korach, K.S., Mendelsohn, M.E., 1997. Estrogen inhibits the vascular injury response in estrogen receptor alpha-deficient mice. Nat. Med. 3, 545–548.

Ikeda, K., Orimo, A., Higashi, Y., Muramatsu, M., Inoue, S., 2000. Efp as a primary estrogen-responsive gene in human breast cancer. FEBS Lett. 472, 9–13.

Inoue, S., Orimo, A., Hosoi, T., Kondo, S., Toyoshima, H., Kondo, T., Ikegami, A., Ouchi, Y., Orimo, H., Muramatsu, M., 1993. Genomic binding-site cloning reveals an estrogen-responsive gene that encodes a RING finger protein. Proc. Natl. Acad. Sci. U.S.A. 90, 11117–11121.

Joyner, J.M., Hutley, L.J., Cameron, D.P., 2001. Estrogen receptors in human preadipocytes. Endocrine 15, 225–230.

Karas, R.H., Hodgin, J.B., Kwoun, M., Krege, J.H., Aronovitz, M., Mackey, W., Gustafsson, J.A., Korach, K.S., Smithies, O., Mendelsohn, M.E., 1999. Estrogen inhibits the vascular injury response in estrogen receptor beta-deficient female mice. Proc. Natl. Acad. Sci. U.S.A. 96, 15133–15136.

Karas, R.H., Schulten, H., Pare, G., Aronovitz, M.J., Ohlsson, C., Gustafsson, J.A., Mendelsohn, M.E., 2001. Effects of estrogen on the vascular injury response in estrogen receptor alpha, beta (double) knockout mice. Circ. Res. 89, 534–539.

Kawabata, W., Suzuki, T., Moriya, T., Fujimori, K., Naganuma, H., Inoue, S., Kinouchi, Y., Kameyama, K., Takami, H., Shimosegawa, T., Sasano, H., 2003. Estrogen receptors (alpha and beta) and 17beta-hydroxysteroid dehydrogenase type 1 and 2 in thyroid disorders: possible in situ estrogen synthesis and actions. Mod. Pathol. 16, 437–444.

Konstantinopoulos, P.A., Kominea, A., Vandoros, G., Sykiotis, G.P., Andricopoulos, P., Varakis, I., Sotiropoulou-Bonikou, G., Papavassiliou, A.G., 2003. Oestrogen receptor beta (ERbeta) is abundantly expressed in normal colonic mucosa, but declines in colon adenocarcinoma paralleling the tumour's dedifferentiation. Eur. J. Cancer 39, 1251–1258.

Kramer, P.R., Wray, S., 2002. 17-Beta-estradiol regulates expression of genes that function in macrophage activation and cholesterol homeostasis. J. Steroid. Biochem. Mol. Biol. 81, 203–216.

Kuiper, G.G., Enmark, E., Pelto-Huikko, M., Nilsson, S., Gustafsson, J.A., 1996. Cloning of a novel receptor expressed in rat prostate and ovary. Proc. Natl. Acad. Sci. U.S.A. 93, 5925–5930.

Matsuyama, S., Ohkura, Y., Eguchi, H., Kobayashi, Y., Akagi, K., Uchida, K., Nakachi, K., Gustafsson, J.A., Hayashi, S., 2002. Estrogen receptor beta is expressed in human stomach adenocarcinoma. J. Cancer Res. Clin. Oncol. 128, 319–324.

Mosselman, S., Polman, J., Dijkema, R., 1996. ER beta: identification and characterization of a novel human estrogen receptor. FEBS Lett. 392, 49–53.

Orimo, A., Inoue, S., Ikeda, K., Noji, S., Muramatsu, M., 1995. Molecular cloning, structure, and expression of mouse estrogen-responsive finger protein Efp. Co-localization with estrogen receptor mRNA in target organs. J. Biol. Chem. 270, 24406–24413.

Orimo, A., Inoue, S., Minowa, O., Tominaga, N., Tomioka, Y., Sato, M., Kuno, J., Hiroi, H., Shimizu, Y., Suzuki, M., Noda, T., Muramatsu, M., 1999. Underdeveloped uterus and reduced estrogen responsiveness in mice with disruption of the estrogen-responsive finger protein gene, which is a direct target of estrogen receptor alpha. Proc. Natl. Acad. Sci. U.S.A. 96, 12027–12032.

Saurin, A.J., Borden, K.L., Boddy, M.N., Freemont, P.S., 1996. Does this have a familiar RING? Trends Biochem. Sci. 21, 208–214.

Sullivan Jr., T.R., Karas, R.H., Aronovitz, M., Faller, G.T., Ziar, J.P., Smith, J.J., O'Donnell Jr., T.F., Mendelsohn, M.E., 1995. Estrogen inhibits the response-to-injury in a mouse carotid artery model. J. Clin. Invest. 96, 2482–2488.

Suzuki, T., Nakamura, Y., Moriya, T., Sasano, H., 2003. Effects of steroid hormones on vascular functions. Microsc. Res. Tech. 60, 76–84.

Takeyama, J., Suzuki, T., Inoue, S., Kaneko, C., Nagura, H., Harada, N., Sasano, H., 2001. Expression and cellular localization of estrogen receptors alpha and beta in human fetus. J. Clin. Endocrinol. Metab. 86, 2258–2262.

Taylor, A.H., Al-Azzawi, F., 2000. Immunolocalisation of oestrogen receptor beta in human tissues. J. Mol. Endocrinol. 24, 145–155.

Thomson, S.D., Ali, S., Pickles, L., Taylor, J., Pace, P.E., Lymboura, M., Shousha, S., Coombes, R.C., 2001. Analysis of estrogen-responsive finger protein expression in benign and malignant human breast. Int. J. Cancer 91, 152–158.

Tokunaga, K., Nakamura, Y., Sakata, K., Fujimori, K., Ohkubo, M., Sawada, K., Sakiyama, S., 1987. Enhanced expression of a glyceraldehyde-3-phosphate dehydrogenase gene in human lung cancers. Cancer Res. 47, 5616–5619.

Tsai, M.J., O'Malley, B.W., 1994. Molecular mechanisms of action of steroid/thyroid receptor superfamily members. Ann. Rev. Biochem. 63, 451–486.

Tsurusaki, T., Aoki, D., Kanetake, H., Inoue, S., Muramatsu, M., Hishikawa, Y., Koji, T., 2003. Zone-dependent expression of estrogen receptors alpha and beta in human benign prostatic hyperplasia. J. Clin. Endocrinol. Metab. 88, 1333–1340.

Urano, T., Saito, T., Tsukui, T., Fujita, M., Hosoi, T., Muramatsu, M., Ouchi, Y., Inoue, S., 2002. Efp targets 14-3-3σ for proteolysis and promotes breast tumour growth. Nature 417, 871–875.

Decreased Expression of 14-3-3σ Is Associated with Advanced Disease in Human Epithelial Ovarian Cancer: Its Correlation with Aberrant DNA Methylation

Jun-ichi Akahira,[1,2] Youko Sugihashi,[1] Takashi Suzuki,[2] Kiyoshi Ito,[1] Hitoshi Niikura,[1] Takuya Moriya,[2] Makoto Nitta,[3] Hitoshi Okamura,[3] Satoshi Inoue,[4] Hironobu Sasano,[2] Kunihiro Okamura,[1] and Nobuo Yaegashi[1]

Departments of [1]Obstetrics and Gynecology, and [2]Pathology, Tohoku University Graduate School of Medicine, Sendai, Japan; [3]Department of Obstetrics and Gynecology, Kumamoto University School of Medicine, Kumamoto, Japan; and [4]Division of Gene Regulation and Signal Transduction, Research Center for Genomic Medicine, Saitama Medical School, Saitama, Japan

ABSTRACT

Purpose: **In this study, we examined the promoter methylation status and expression of 14-3-3σ and evaluated its clinical significance in epithelial ovarian cancer.**

Experimental Design: **Twelve ovarian cancer cell lines; 2 ovarian surface epithelial cell lines; and 8 normal, 8 benign, 12 borderline, and 102 ovarian cancer tissues were examined. Methylation-specific PCR, quantitative reverse transcription-PCR, and immunohistochemistry were used to evaluate methylation status and expression of *14-3-3σ* gene and protein.**

Results: **Among the 12 ovarian cancer cell lines, the presence of a methylated band was detected in seven cell lines. Median values of relative *14-3-3σ* gene expression in cancers with methylation (3.27) were significantly lower than those without methylation (16.4; $P < 0.001$). Treatment of 5-aza-2′-deoxycitidine resulted in the demethylation of the promoter CpG islands and reexpression. All of the normal, benign, and borderline tissues were positive for 14-3-3σ protein, and in ovarian cancer tissues, 73.5% (75 of 102) were positive for 14-3-3σ protein and was almost consistent with methylation status. Negative immunoreactivity of 14-3-3σ was significantly correlated with high age and serous histology, high-grade, advanced-stage residual tumor of >2 cm, high serum CA125, high Ki-67 labeling index, and positive p53 immunoreactivity. 14-3-3σ immunoreactivity was significantly associated with overall survival ($P = 0.0058$).**

Conclusions: **Our findings suggest that 14-3-3σ is inactivated mainly by aberrant DNA methylation and that it may play an important role in the pathogenesis of epithelial ovarian cancer.**

INTRODUCTION

Epithelial ovarian cancer is the leading cause of death from gynecological malignancies in the great majority of developed countries (1). This high mortality is considered to be, in large part, due to the advanced stage of the disease commonly present at the time of diagnosis, but many clinical studies have reported that there are some prognostic factors in ovarian cancer other than clinical stages, such as histology, the degree of primary surgical cytoreduction, and response to chemotherapy (1–3). Other prognostic parameters have been also proposed in addition to those relatively established parameters. These include Ki67 index, progesterone receptor, and the preoperative serum maker CA125, and others (4–6). The identification of new prognostic factors may further contribute to improve treatment and clinical outcome of ovarian cancer patients.

The cause of epithelial ovarian cancer is still unknown. Although *BRCA1* and *BRCA2* mutation have been identified as associated with susceptibility to ovarian cancer (7, 8), mutations in these genes account for only 2–3% of all ovarian cancers. The remaining cases are considered to be sporadic in nature and arise as a result of acquired alterations in oncogenes and tumor suppressor genes such as *TP53* and *PTEN* (9–11).

DNA methylation has an essential regulatory function in mammalian development, suppressing gene activity by changing chromatin structure (12, 13). It has become apparent that aberrant DNA methylation of promoter region CpG islands may serve as an alternate mechanism to genetic defects in the inactivation of tumor suppressor genes in human cancers (14, 15). Accordingly, the identification of gene targets of methylation-associated silencing could lead to novel genes involved in the initiation and progression of human neoplasia.

14-3-3σ was originally identified as a p53-inducible gene that is responsive to DNA damaging agents (16). Recent study demonstrated that 14-3-3σ protein plays a crucial role in the G_2 checkpoint by sequestering the mitotic initiation complex, cdc2-cyclin B1, in the cytoplasm after DNA damage (17). This prevents cdc2-cyclin B1 from entering the nucleus in which the protein complex would normally initiate mitosis. In this manner, 14-3-3σ induces G_2 arrest and allows the repair of damaged DNA (16, 17). The expression of 14-3-3σ is reported to be frequently lost in human breast, gastric, and lung cancers, and the inactivation is due to

Received 10/31/03; revised 12/3/03; accepted 12/19/03.
Grant support: Supported in part by a grant-in-aid for Scientific Research from the Ministry of Health and Welfare, a grant-in-aid from the Ministry of Education, Science and Culture, a grant-in-aid from Kurokawa Cancer Research Foundation, and a grant-in-aid from Japan Society of Gynecologic Oncology (JSGO).
The costs of publication of this article were defrayed in part by the payment of page charges. This article must therefore be hereby marked *advertisement* in accordance with 18 U.S.C. Section 1734 solely to indicate this fact.
Requests for reprints: Jun-ichi Akahira, Department of Obstetrics and Gynecology, Tohoku University Graduate School of Medicine, 1-1 Seiryo-machi, Aoba-ku, Sendai, 980-8574, Japan. Phone: 81-22-717-7254; Fax: 81-22-717-7258; E-mail: jakahira-tohoku@umin.ac.jp.

aberrant DNA methylation (18–20). However, the expression of 14-3-3σ and its mechanism have not been examined in epithelial ovarian cancer. Therefore, in this study, we examined the promoter methylation status and expression of 14-3-3σ in epithelial ovarian cancer cells. We also evaluated the correlation between 14-3-3σ expression and clinicopathological parameters in patients with epithelial ovarian cancer.

MATERIALS AND METHODS

Tissues and Cells. Eight normal ovaries, 8 ovarian serous cystadenomas, 12 serous borderline tumors, and 102 ovarian cancer cases were obtained from patients after surgical therapy from 1988 to 2000 at Tohoku University Hospital, Sendai, Japan. In ovarian cancer patients, information regarding age, performance status on admission, histology, stage, grade, residual tumor after primary surgery, and overall survival were retrieved from the review of patient charts. Median follow-up time of the patients in this study was 59 months (4–120 months). Eighty-four (82.3%) of 102 patients received platinum-containing chemotherapy after operation. Patients who have early-stage (stage Ia) and low grade-disease (G1, G2) and patients who have poor performance status did not receive platinum-based chemotherapy. Performance status was defined according to WHO criteria (21). Histology and stage were determined according to FIGO (International Federation of Gynecology and Obstetrics) criteria. Grade was evaluated by one of the authors (T. M.) using universal grading system in epithelial ovarian cancer (22). Residual disease was determined by the amount of unresectable tumor that remained after primary cytoreductive surgery. Optimal cytoreduction was defined as no gross residual tumor greater than 2 cm in diameter, and suboptimal cytoreduction was defined as any gross residual disease remaining greater than 2 cm in diameter. Overall survival was calculated from the time of initial surgery to death, or the date of last contact. Survival times of patients still alive or lost to follow-up were censored in December 2002. All of these archival specimens were retrieved from the surgical pathology files at Tohoku University Hospital, Sendai, Japan. These specimens were all fixed in 10% formalin and embedded in paraffin. The research protocol was approved by the ethics committee of Tohoku University Graduate School of Medicine.

OVCAR3, Caov3, SKOV3, TOV112D, TOV21G, OV90, and ES2 (adenocarcinoma, OVCAR3, SKOV3; serous adenocarcinoma, Caov3, OV90; clear cell adenocarcinoma, TOV21G, ES2; endometrioid adenocarcinoma, TOV112D) cell lines were purchased from American Type Culture Collection. JHOS2, JHOS3, HTOA, OMC3, and JHOC5 (serous adenocarcinoma, JHOS2, JHOS3, HTOA; mucinous adenocarcinoma, OMC3; clear cell adenocarcinoma, JHOC5) cell lines were purchased from Riken cell bank (Tsukuba, Japan). Normal ovarian surface epithelial cell lines (OSE2 and OSE4) were established by one of the authors (M. N.; Ref. 23). Cell lines were maintained in DMEM/F12 (Invitrogen) supplemented with 10% fetal bovine serum and 1% penicillin/streptomycin (Invitrogen), and were incubated in 5% CO_2 at 37°C. For 5-aza-2′ deoxycytidine (5azaC) treatment, 1×10^6 cells were seeded into T75 flasks and were treated with 0.5 μM or 1.0 μM 5azaC (Sigma) for 72 h.

Methylation-Specific PCR. Methylation status of the samples was investigated by methylation-specific PCR as described in the literature (24). Genomic DNA of ovarian cancer tissue was extracted using a laser capture microdissection and treated with proteinase K (0.5 mg/ml) for 48 h at 37°C. Genomic DNA from ovarian cancer cell lines was extracted using Aqua-Pure Genomic DNA kit (Bio-Rad). The quality and integrity of the DNA was determined by the A260:280 ratio. One μg of genomic DNA was treated with sodium bisulfite using CpGenome DNA modification kit (Intergen) according to the instructions. Amplification was achieved in a 20-μl reaction volume containing 2 μl of 10× Ex Taq Buffer, 1.5 μl of 25 mM $MgCl_2$, 1 μM each primer, 1.5 μl of 2.5 mM dNTPs, and 1 unit of Takara Ex Taq polymerase (Takara, Japan). Hot-start PCR was performed in a thermal cycler (Takara) for 35 cycles, each of which consisted of denaturation at 96°C for 30 s, annealing at 64°C for 30 s, and extension at 72°C for 90 s, followed by a final 10 min extension at 72°C. Primers used were 5′-TGGTAG-TTTTTATGAAAGGCGTC-3′ and 5′-CCTCTAACCGCCCA-CCACG-3′ (104-bp) for the methylated reaction (M primers), and 5′-ATGGTAGTTTTTATGAAAGGTGTT-3′ and 5′-CCCT-CTAACCACCCACCACA-3′ (106-bp) for the unmethylated reaction (U primers; Ref. 18). Universal methylated human male genomic DNA (Intergen) was used as a positive control for methylated reaction. Genomic DNA purified from MCF-7 breast cancer cell line was used as a positive control for unmethylated reaction (18). A blank control containing all of the PCR components except template DNA was also included in all of the PCRs. Reaction products were separated by electrophoresis on a 3% agarose gel, stained with ethidium bromide, and visualized under UV illumination. Specimens with purely unmethylated promoters have positive PCR products by U primers but not with the M primers. Specimens that contain purely methylated promoters will have PCR products by using M primers but not with the U primers. Specimens that contain heterogeneous status of both methylated and unmethylated promoters have PCR products from both U primers and M primers.

Reverse Transcription and Real-Time Quantitative PCR. Total RNA was isolated from cell lines by phenol-chloroform extraction using Isogen (Nippon Gene, Tokyo, Japan). RNA was treated with RNase-free DNase (Roche Diagnostics; 1 μg/μl) for 2 h at 37°C, followed by heat inactivation at 65°C for 10 min. A reverse transcription-PCR kit (SUPERSCRIPT II First-strand synthesis system, Invitrogen) was used and cDNA synthesis was carried out according to the instructions. cDNAs were synthesized from 2 μg of total RNA using random hexamer, and reverse transcription was carried out for 50 min at 42°C with SUPERSCRIPT II reverse transcriptase. Real-time quantitative PCR was performed using the iCycler system (Bio-Rad). For the determination of 14-3-3σ cDNA content, a 25-μl reaction mixture consisted of 23 μl iQ SYBR Green MasterMix, 1 μM each primer, and 1 μl of template cDNA were prepared. The PCR conditions were as follows: initial duration at 96°C for 60 s, and followed by 35 cycles with denaturation at 96°C for 30 s, annealing at 64°C (both for 14-3-3σ and β-actin) for 30 s, and extension at 72°C for 30 s. The fluorescence intensity of the double-strand specific SYBR Green I, reflecting the amount of formed PCR-product, was read at 88°C after the end of each elongation step. Primers used were

as follows: 14-3-3σ, 5′-CCTGCTGGACAGCCACCTCA-3′ and 5′-TGTCGGCCGTCCACAGTGTC-3′ (397-bp; Ref. 20); β-actin, 5′-CCAACCGCGAGAAGATGA-3′ and 5′-GGAAGGAAGGCTGGAAGAGT-3′ (459-bp; Ref. 25). β-actin cDNA fragments were amplified as internal positive controls. Normal human ovarian cDNA library (Stratagene, La Jolla, CA) was used as a normal control, cDNA from MCF-7 was used as a positive control, and water blank was used as a negative PCR control (data not shown). Control reactions in which reverse transcriptase was omitted were amplified under the same conditions to exclude DNA contamination (data not shown). Two independent quantitative PCR reactions were performed for each sample.

Immunohistochemistry. Immunohistochemical analysis was performed using the streptavidin-biotin amplification method using a Histofine kit (Nichirei, Tokyo, Japan), and have been previously described in detail (26). Polyclonal antibody for 14-3-3σ (N-14), monoclonal antibody for p53 (B20.1), and monoclonal antibody for Ki-67 (MIB-1) were purchased from Santa Cruz Biotechnology, Inc. (Santa Cruz, CA), Biomeda (Foster City, CA), and DAKO (Tokyo, Japan), respectively.

For antigen retrieval, the slides were heated in an autoclave at 120°C for 5 min in citric acid buffer [2 mM citric acid and 9 mM trisodium citrate dyhydrate (pH 6.0)]. The dilutions of primary antibodies for 14-3-3σ, p53 and Ki-67 were 1:100, 1:40, and 1:300, respectively. The antigen-antibody complex was visualized with 3,3′-diaminobenzidine (DAB) solution [1 mM DAB, 50 mM Tris-HCl buffer (pH 7.6), and 0.006% H_2O_2], and counterstained with hematoxylin. Nonneoplastic breast epithelial tissue was used as a positive control (18). As negative controls, 0.01 M PBS and normal mouse IgG were used in place of primary antibodies.

The immunohistochemical expression of 14-3-3σ, p53, and Ki-67 was independently reviewed by two of the authors (J. A. and T. M.) who had no knowledge of the clinicopathological data. As immunoreactivities of 14-3-3σ and p53 were relatively homogeneous and clearly distinguished for positive and negative, they were classified into two groups: +, positive carcinoma cells; and −, no immunoreactivity. Scoring of Ki-67 in carcinoma cells was counted independently by these same two authors, and the percentage of immunoreactivity in at least 500 carcinoma cells, *i.e.*, labeling index, was determined. Whenever a difference of greater than 5% was observed between the two readings, slides were reviewed jointly, and a consensus was reached.

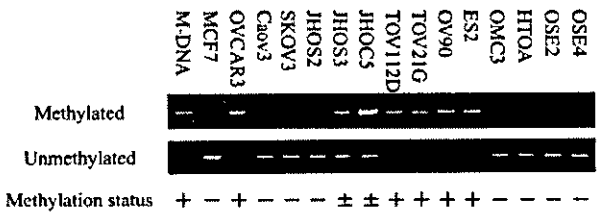

Fig. 1 Methylation-specific PCR (MSP) for 14-3-3σ in ovarian cancer and surface epithelial cell lines. Specimens with methylated promoters have positive PCR products in the *Methylated Lane*, and specimens with unmethylated promoters have positive PCR products in the *Unmethylated Lane*. Specimens that contain heterogeneous status of both methylated and unmethylated promoters have PCR products in both the *Methylated* and the *Unmethylated Lanes*. Methylation statuses of each cell line are defined as; +, purely methylated: −, purely unmethylated: ±, both methylated and unmethylated, and are shown in the *Methylation status Lane*. *M-DNA* (universal methylated human male genomic DNA) was used as a positive control for methylated reaction. MCF-7 (*MCF7*) breast cancer cell line was used as a positive control for unmethylated reaction.

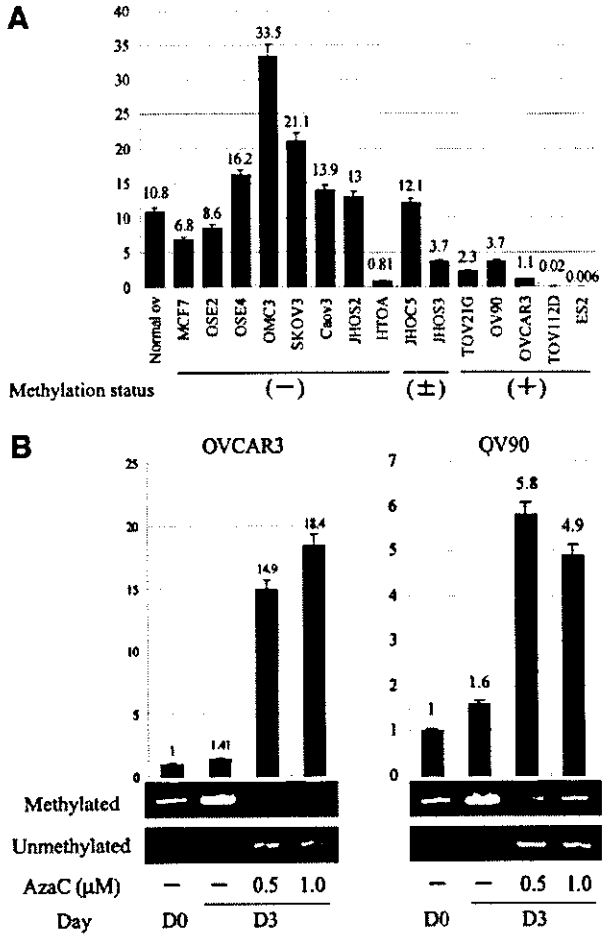

Fig. 2 *A*, expression of the *14-3-3σ* gene in ovarian cancer cells. Mean of the two independent results of real-time quantitative reverse transcription (RT)-PCR of ovarian cancer and surface epithelial cell lines are shown. *The number on top of each bar*, relative *14-3-3σ* gene expression standardized by the amount of internal positive control (β-actin). Normal ov (normal human ovarian cDNA library) was used as a normal control. MCF-7 was used as a positive control. *B*, reexpression of the *14-3-3σ* gene by 5-aza-2′-deoxycitidine (5azaC) treatment. OVCAR3 and OV90 cell lines that have only methylated bands were treated with 5azaC for 3 days. Methylation status and mRNA expression of 14-3-3σ was assessed by methylation-specific PCR (MSP) and quantitative RT-PCR on day 0 (*D0*) and day 3 (*D3*) with or without 5azaC (0.5 μM and 1.0 μM) treatment (*AzaC*). Complete and partial demethylation was observed in OVCAR3 and OV90, respectively. *The number on the top of each bar*, relative *14-3-3σ* gene expression standardized by the amount of internal positive control (β-actin).

Statistical Analysis. Statistical analysis was performed using Stat View 5.0 (SAS Institute Inc.) software. The statistical significance between 14-3-3σ and characteristics of the patients was evaluated using Mann-Whitney *U* test, Kruskal-Wallis test, and Scheffe analysis. Correlation between 14-3-3σ and Ki-67, p53 immunoreactivity was also assessed using Mann-Whitney

U test. Univariate analysis of prognostic significance for prognostic factors was performed using a log-rank test, after each survival curve was obtained by the Kaplan-Meier method. Multivariate analysis was performed using Cox regression model to evaluate the predictive power of each variable independently of the others. All of the patients who could be assessed were included in the intention-to-treat analysis. A result was considered significant when the P was less than 0.05.

RESULTS

Methylation Status and Expression of 14-3-3σ in Ovarian Cancer Cells. Among the 12 ovarian cancer cell lines in which 14-3-3σ promoter methylation was investigated, the presence of a methylated band was detected in 7 cell lines, 2 of which were together with unmethylated band as shown in Fig. 1. The methylated band was detected in all of the cell lines derived from clear cell adenocarcinoma (TOV21G, ES2, JHOC5), two of five of serous adenocarcinoma (Caov3, OV90, JHOS2, JHOS3, HTOA), one of one of endometrioid adenocarcinoma (TOV112D), and none of one of mucinous adenocarcinoma (OMC-3). Both of the OSE cells were negative for methylated band.

The expression of *14-3-3σ* gene is shown in Fig. 2*A*. Quantitative reverse transcription-PCR was performed and the ratio of 14-3-3σ:β-actin was calculated to allow for comparison between the cell lines. Median values of relative *14-3-3σ* gene expression in cancers with methylation (3.27) were significantly lower than those without methylation (16.4; $P < 0.001$, Kruskal-Wallis test). In HTOA, the expression of *14-3-3σ* gene was relatively decreased, although this cell line did not have methylated promoter alleles. The expression of *14-3-3σ* gene was relatively high in OSE2 (8.6), OSE4 (16.2), and in the normal ovarian cDNA library (10.8).

To further confirm that aberrant DNA methylation contributed to loss of expression of *14-3-3σ* gene, we assessed the effect of 5azaC, a demethylating agent, on 14-3-3σ mRNA expression by quantitative reverse transcription-PCR. Treatment of OVCAR3 and OV90 cells with 5azaC for 3 days resulted in the complete and partial demethylation of the promoter CpG islands and reexpression of *14-3-3σ* gene, respectively (Fig. 2*B*). The amount of expression of mRNA after treatment (14.9 and 5.8 for 0.5 μM, and 18.4 and 4.9 for 1.0 μM in OVCAR and OV90, respectively) was significantly higher than that before

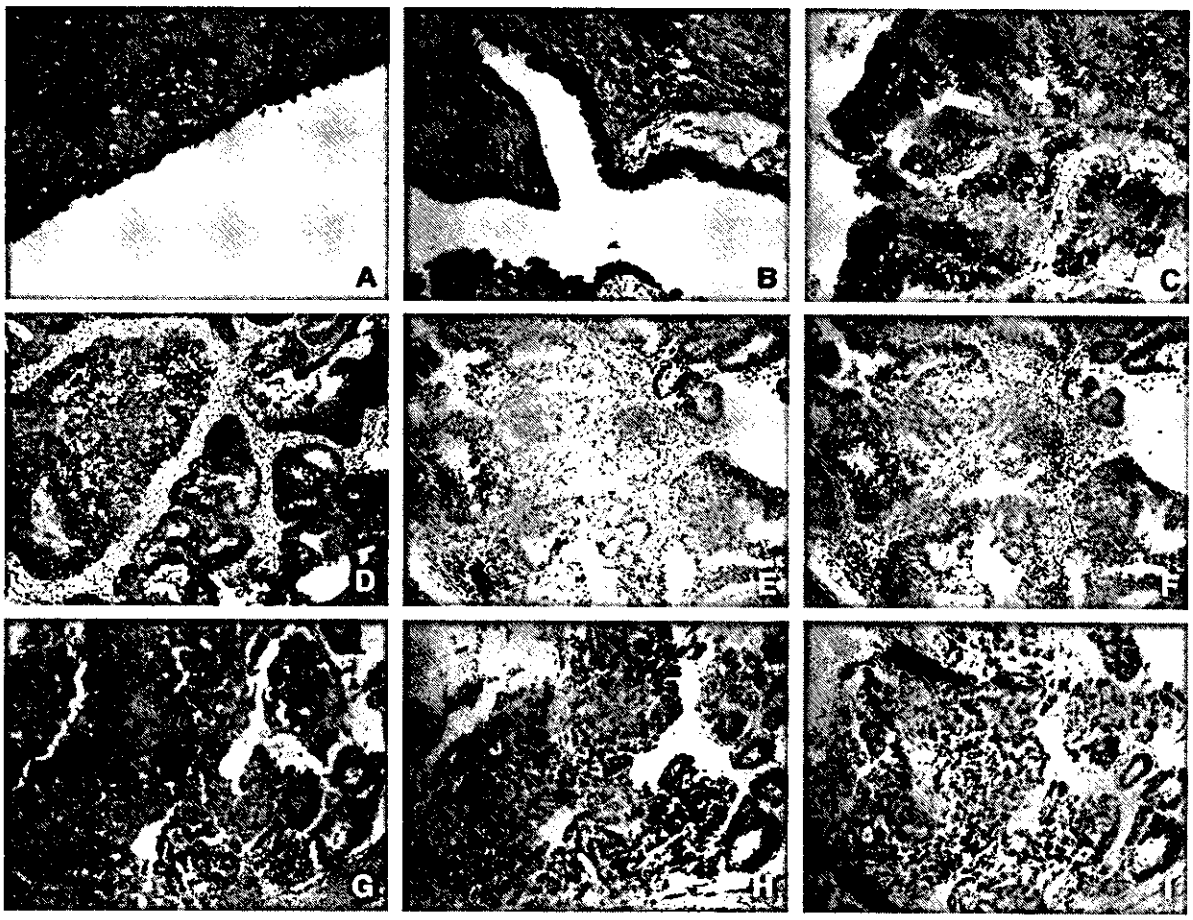

Fig. 3 Immunohistochemistry for 14-3-3σ in normal ovary, and in benign, borderline, and malignant ovarian tumors. Representative cases of immunohistochemistry for 14-3-3σ in the ovarian surface epithelium (*A*), benign adenoma (*B*), borderline tumor (*C*), two cases of epithelial ovarian cancer (*D, G*), and serial sections of each case for Ki-67 (*E, H*) and p53 (*F, I*) are shown. Note that positive 14-3-3σ case (*D*) is negative for Ki-67 (*E*) and p53 (*F*), whereas negative 14-3-3σ case (*G*) is positive for Ki-67 (*H*) and p53 (*I*), ×200 for all figures.

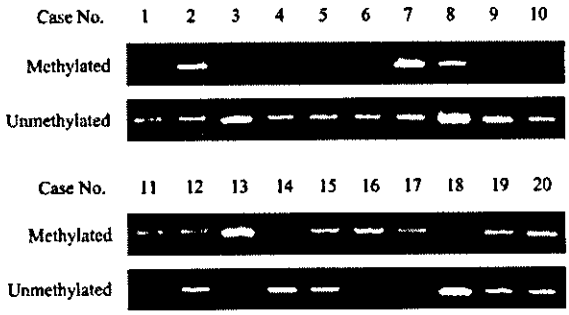

Fig. 4 Methylation-specific PCR (MSP) for *14-3-3σ* gene in ovarian cancer tissues. The methylation status of *14-3-3σ* gene in microdissected ovarian cancer tissues was evaluated by MSP in the 10 cases of positive (*Lanes 1–10*), and 10 cases of negative (*Lanes11–20*) immunoreactivity. Definition of *Methylated* and *Unmethylated Lanes* are the same as in Fig. 1.

treatment ($P < 0.001$, Kruskal-Wallis test). The decreased expression of 14-3-3σ in this cell line is, therefore, not attributable to abnormalities at the gene level or to the inability to express 14-3-3σ, but rather is directly related to the methylation.

Immunohistochemistry and Methylation Status of 14-3-3σ in Ovarian Cancer Tissues. Positive immunoreactivity for 14-3-3σ was detected in the cytoplasm of epithelial cells, although p53 and Ki-67 were confined exclusively to the nuclei of epithelial cells (Fig. 3). In normal, benign, and borderline tissues, all of the cases were positive for 14-3-3σ immunoreactivity. In ovarian cancer tissues, 73.5% (75 of 102) and 36.3% (37 of 102) were positive for 14-3-3σ and p53, respectively. Median Ki-67 labeling index was 17.2%.

To further clarify the relationships between 14-3-3σ immunoreactivity and aberrant DNA methylation in ovarian cancer tissues, we analyzed the methylation status in microdissected ovarian cancer tissues (Fig. 4). In the 10 cases of positive immunoreactivity, unmethylated bands were detected in all of the cases, and methylated bands were detected in 3 cases. In the another 10 cases of negative immunoreactivity, methylated bands were detected in 8 cases, although only unmethylated bands were detected in 2 cases.

Correlation between Clinicopathological Parameters and Immunohistochemistry in Ovarian Cancer Patients. Results of immunohistochemistry for 14-3-3σ, p53, and Ki-67 and correlation with clinicopathological parameters are summarized in Table 1. Negativity of 14-3-3σ was significantly correlated with high age, serous histology, high-grade, advanced-stage, residual tumor of >2 cm, high serum CA125, and high Ki-67 labeling index. Interestingly, p53 expression was inversely correlated with that of 14-3-3σ.

Results of univariate analysis of prognostic significance for

Table 1 Correlation between 14-3-3 σ immunoreactivity and clinicopathological parameters in epithelial ovarian cancer

			14-3-3 σ immunoreactivity		
	Total (n = 102)	%	+ (n = 75)	− (n = 27)	P
Age (median)	51		48.3	60.4	0.039
≦50	50	49.0	41	9	
>50	52	51.0	34	18	
Performance status[a]					
0–1	72	70.6	56	16	0.13
2–4	30	29.4	19	11	
Histology					
Serous	45	44.1	24	21	0.0003
Endometrioid	16	15.7	14	2	
Mucinous	14	13.7	14	0	
Clear cell	27	26.5	23	4	
Grade					
1	43	42.2	39	4	0.0022
2	35	34.3	23	12	
3	24	23.5	13	11	
Stage					
I/II	48	47.1	45	3	0.0001
III/IV	54	52.9	30	24	
Residual tumor[b]					
≦2 cm	62	60.8	55	7	0.0001
>2 cm	40	39.2	20	20	
CA125 (median, IU/liter)	255		43.5	63.9	0.0016
p53 immunoreactivity					
Positive	37	36.3	21	16	0.0038
Negative	65	63.7	54	11	
Ki67 LI (median)	17.2		15.6	24.4	0.047

[a] Performance status score: 0, asymptomatic and fully active; 1, symptomatic, fully ambulatory, restricted in physically strenuous activity; 2, symptomatic, ambulatory, capable of self-care, more than 50% of waking hours are spent out of bed; 3, symptomatic, limited self-care, spends more than 50% of time in bed, but not bedridden; 4, completely disabled, no self-care, bedridden.

[b] Residual tumor is defined in the "Materials and Methods."

[c] LI, labeling index.

Table 2 Univariate analysis of overall survival in epithelial ovarian cancer

Variable	*P*
14-3-3 σ (positive *vs.* negative)	0.0058
Age (≦50, >50)	0.029
PS[a] (0–1 *vs.* 2–4)	<0.0001
Histological type	0.913
Histological grade	0.05
Stage (I/II *vs.* III/IV)	<0.0001
Residual tumor (≤2 cm *vs.* >2 cm)	<0.0001
p53 (positive *vs.* negative)	0.36
Ki67 (<15% *vs.* >15%)	0.011

[a] PS, performance status.

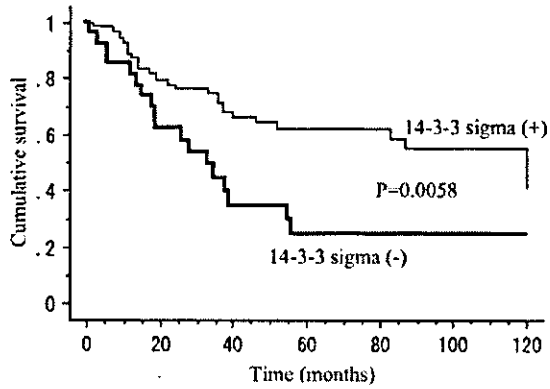

Fig. 5 Correlation between 14-3-3σ expression and overall survival in patients with epithelial ovarian cancer.

each variable with respect to survival are summarized in Table 2. In this analysis, we determined the positive cases of Ki-67 as those with a labeling index of more than 15%. Among the clinicopathological factors examined, those significantly associated with overall survival were 14-3-3σ immunoreactivity, age, performance status, grade, stage, residual tumor, and Ki-67. Negative 14-3-3σ cases had significantly worse overall survival rates than positive cases (Fig. 5; $P = 0.0058$). In multivariate analysis, 14-3-3σ immunoreactivity turned out not to be an independent prognostic indicator (Table 3). Among the variables examined, only stage and residual tumor turned out to be independent prognostic factors.

DISCUSSION

The aberrant methylation of 14-3-3σ was associated with loss of RNA expression, and the expression was restored by treatment with the demethylating agent 5azaC, indicating that aberrant DNA methylation is the main pathway of transcriptional silencing of *14-3-3σ* gene in ovarian cancer cells. Also, decreased expression of 14-3-3σ occurs in substantial proportion, and it turned out to be a prognostic factor in univariate analysis in epithelial ovarian cancer tissues. These results suggest the importance of the *14-3-3σ* gene in the development and progression of this tumor. To our knowledge, this is the first report on epigenetic silencing of 14-3-3σ in human ovarian cancer.

The *14-3-3σ* gene is demonstrated to be induced after DNA damage in a p53-dependent manner (16), and to play a role in the G_2 checkpoint by sequestering the Cdc2/cyclin B1 complex (17). Similar to our results, several authors demonstrated epigenetic inactivation of the *14-3-3σ* gene in human cancers (18, 20, 27). Experimental inactivation of the *14-3-3σ* gene causes a G_2 checkpoint defect, and results in the accumulation of chromosomal aberrations that increase the sensitivity to the DNA-damaging events (28, 29). In this context, it is of interest that serous histology in which significantly decreased expression of 14-3-3σ protein was observed is highly sensitive to chemotherapeutic agents. The histological type-specific expression of the *14-3-3σ* gene suggests that serous adenocarcinomas develop unique differentiation, different from other histological subtypes. Although a high proportion of human cancers are likely to have a chromosomal instability phenotype, mutations of the genes involving the G_2-M-phase checkpoint have rarely been found, and the mechanism of chromosomal instability in most of them is still unknown. Further study on the correlation between genetic instability and 14-3-3σ is needed.

In a number of previous reports, it is strongly postulated that the inactivation of 14-3-3σ might play an important role in tumor progression. Ostergaard *et al.* (30) showed that less-differentiated bladder squamous cell carcinoma is characterized by decreased expression of some proteins, including 14-3-3σ. Suzuki *et al.* (19) reported that aberrant methylation of the *14-3-3σ* gene was frequently observed in poorly differentiated gastric adenocarcinoma. Umbricht *et al.* (31) reported that decreased expression of 14-3-3σ was observed in 24 (96%) of 25 carcinomas, 15 (83%) of 18 of ductal carcinoma *in situ*, and 3 (38%) of 8 of atypical hyperplasias, and concluded that inactivation of 14-3-3-sigma occurs at an early stage in the progression of invasive breast cancer. Osada *et al.* (20) recently demonstrated frequent and type-specific inactivation of the *14-3-3σ* gene in small cell lung cancer. In our study, loss of 14-3-3σ expression was significantly correlated with high-grade advanced-stage bulky residual tumor and high serum CA125 and high Ki-67 levels, all of these factors represent fundamental difference in pathogenesis in ovarian cancer. Our results, together with previous reports, suggest that the loss of 14-3-3σ expression in ovarian cancer may have invasive and progressive characteristics.

Recent study suggests that promoter methylation increases with age in several genes in normal tissues, although the mechanism of age-related methylation is unknown (32, 33). Several factors may modulate age-related methylation, such as exogenous carcinogens, endogenously generated reactive oxygen species, and genetic differences in individual susceptibility (33). In our study, 14-3-3σ protein expression was decreased in elderly

Table 3 Multivariate analysis of overall survival using Cox's proportional hazard model

Variable	*P*
14-3-3 σ (positive *vs.* negative)	0.34
Age (≦50, >50)	0.15
PS[a] (0–1 *vs.* 2–4)	0.29
Histological grade	0.73
Stage (I/II *vs.* III/IV)	0.0081
Residual tumor (≤2 cm *vs.* >2 cm)	0.023
Ki67 (<15% *vs.* >15%)	0.11

[a] PS, performance status.

patients by immunohistochemistry. Although age-related methylation of *14-3-3σ* has not been reported, it is possible that expression of this gene is suppressed by methylation with age, and it may contribute to carcinogenesis in ovarian cancer.

In the present study, a clear correlation between aberrant methylation and silencing of 14-3-3σ was observed except for one cell line (HTOA) and 2 of 10 primary ovarian cancer tissues, which showed unmethylated patterns despite loss of 14-3-3σ expression. These results suggest that DNA methylation-independent mechanism may also be involved in the loss of 14-3-3σ expression. Several other ways of gene inactivation such as loss of transcription factor are assumed, and Osada *et al.* (20) considered that *14-3-3σ* gene silencing might occur without methylation in only primary tissues. From our results, positive p53 immunoreactivity, which suggests loss of functional p53 protein (34, 35), seems to contribute to the loss of 14-3-3σ expression in primary ovarian tissues. Possible methylation-independent mechanism remains to be elucidated to better understand the regulation of 14-3-3σ expression.

In conclusion, aberrant CpG island methylation is an epigenetic change that is largely responsible for silencing of the *14-3-3σ* gene. Inactivation of 14-3-3σ occurs in substantial proportion and may play a role as a potential tumor suppressor gene in epithelial ovarian cancer.

REFERENCES

1. Akahira J, Yoshikawa H, Shimizu Y, et al.Prognostic factors of stage IV epithelial ovarian cancer: a multicenter retrospective study. Gynecol Oncol 2001;81:398–403.
2. Del Campo JM, Felip E, Rubio D, et al. Long-term survival in advanced ovarian cancer after cytoreduction and chemotherapy treatment. Gynecol Oncol 1994;53:27–32.
3. Omura GA, Brady MF, Homesley HD, et al. Long-term follow-up and prognostic factor analysis in advanced ovarian carcinoma: the gynecologic oncology group experience. J Clin Oncol 1991;9:1138–50.
4. Kaufmann M, Von Minckwitz G, Kuhn W, et al. Combination of new biologic parameters as prognostic index in epithelial ovarian carcinoma. Int J Gynecol Cancer 1995;5:49–55.
5. Akahira J, Inoue T, Suzuki T, et al. Progesterone receptor isoforms A and B in human epithelial ovarian carcinoma: immunohistochemical and RT-PCR studies. Br J Cancer 2000;83:1488–94.
6. Cooper BC, Sood AK, Davis CS, et al. Pre-operative CA125 levels: an independent prognostic factor for epithelial ovarian cancer. Obstet Gynecol 2002;100:59–64.
7. Miki Y, Swensen J, Shattuck-Eidens D, et al. A strong candidate for the breast and ovarian cancer susceptibility gene BRCA1. Science (Wash DC) 1994;266:66–71.
8. Wooster R, Bignell G, Lancaster J, et al. Identification of the breast cancer susceptibility gene BRCA2. Nature (Lond) 1995;378:789–92.
9. Guttmacher AE, Collins FS. Breast and ovarian cancer. N Engl J Med 2003;348:2339–47.
10. Newman B, Millikan RC, King MC. Genetic epidemiology of breast and ovarian cancers. Epidemiol Rev 1997;19:69–79.
11. Ford D, Easton DF, Peto J. Estimates of the gene frequency of BRCA1 and its contribution to breast and ovarian cancer incidence. Am J Hum Genet 1995;57:1457–62.
12. Kass SU, Pruss D, Wolffe AP. How does DNA methylation repress transcription? Trends Genet 1997;13:444–9.
13. Razin A, Ceder H. DNA methylation and gene expression. Microbiol Rev 1991;55:451–8.
14. Jones PA, Laird PW. Cancer epigenetics comes of age. Nat Genet 1999;21:163–7.
15. Esteller M, Corn PG, Baylin SB, Herman JG. A gene hypermethylation profile of human cancer. Cancer Res 2001;61:3225–9.
16. Hermeking H, Lengauer C, Polyak K, et al. 14-3-3σ is a p53-regulated inhibitor of G_2/M progression. Mol Cell 1997;1:3–11.
17. Chan TA, Hermeking H, Langauer C, Kinzler KW, Vogelstein B. 14-3-3σ is required to prevent mitotic catastrophe after DNA damage. Nature (Lond) 1999;401:616–20.
18. Ferguson AT, Evron E, Umbricht CB, et al. High frequency of hypermethylation at the 14-3-3σ locus leads to gene silencing in breast cancer. Proc Natl Acad Sci USA 2000;97:6049–54.
19. Suzuki H, Itoh F, Toyota M, et al. Inactivation of the 14-3-3σ gene is associated with 5′ CpG island hypermethylation in human cancers. Cancer Res 2000;60:4353–7.
20. Osada H, Tatematsu Y, Yatabe Y, et al. Frequent and histological type-specific inactivation of 14-3-3σ in human lung cancers. Oncogene 2002;21:2418–24.
21. WHO. Handbook for reporting results of cancer treatment. WHO Publication No. 48. Geneva: WHO; 1979.
22. Shimizu Y, Kamoi S, Amada S, et al. Toward the development of a universal grading system for ovarian epithelial carcinoma. Prognostic significance of histopathologic features-problems involved in the architectural grading system. Gynecol Oncol 1998;70:2–12.
23. Nitta M, Katabuchi H, Ohtake H, et al. Characterization and tumorigenicity of human ovarian surface epithelial cells immortalized by SV40 large T antigen. Gynecol Oncol 2001;81:10–7.
24. Herman JG, Graff JR, Myohanen S, Nelkin BD, Baylin SB. Methylation-specific PCR: a novel PCR assay for methylation status of CpG islands. Proc Natl Acad Sci USA 1996;93:9821–6.
25. Akahira J, Suzuki T, Ito K, et al. Differential expression of progesterone receptor isoforms A and B in the normal ovary, and in benign, borderline, and malignant ovarian tumors. Jpn J Cancer Res 2002;93: 807–15.
26. Akahira J, Suzuki T, Ito K, et al. Expression of 5α-reductases in human epithelial ovarian cancer: its correlation with androgen receptor status. Jpn J Cancer Res 2001;92:926–32.
27. Lodygin D, Yazdi AS, Sander CA, Herzinger T, Hermeking H. Analysis of 14-3-3σ expression in hyperproliferative skin diseases reveals selective loss associated with CpG-methylation in basal cell carcinoma. Oncogene 2003;22:5519–24.
28. Dhar S, Squire JA, Hande MP, Wellinger RJ, Pandita TK. Inactivation of 14-3-3σ influences telomere behavior and ionizing radiation-induced chromosomal instability. Mol Cell Biol 2000;20:7764–72.
29. Lengauer C, Kinzler KW, Vogelstein B. Genetic instability in human cancers. Nature (Lond) 1999;396:643–9.
30. Ostergaard M, Rasmussen HH, Nielsen HV, et al. Proteome profiling of bladder squamous cell carcinomas: identification of markers that define their degree of differentiation. Cancer Res 1997;57:4111–7.
31. Umbricht CB, Evron E, Gabrielson E, et al. Hypermethylation of 14-3-3σ (stratifin) is an early event in breast cancer. Oncogene 2001; 20:3348–53.
32. Ahuja N, Li Q, Mohan AL, Baylin SB, Issa JP. Aging and DNA methylation in colorectal mucosa and cancer. Cancer Res 1998;58: 5489–94.
33. Issa JP. CpG-island methylation in aging and cancer. Curr Top Microbiol Immunol 2000;249:101–18.
34. Iggo R, Gatter K, Bartek J, Lane D, Harris AL. Increased expression of mutant forms of p53 oncogene in primary lung cancer. Lancet 1990;335:675–9.
35. Skilling JS, Sood A, Niemann T, Lager DJ, Buller RE. An abundance of p53 null mutations in ovarian carcinoma. Oncogene 1996;13: 117–23.

Available online at www.sciencedirect.com
SCIENCE DIRECT®
Biochemical and Biophysical Research Communications 325 (2004) 1312–1317
BBRC
www.elsevier.com/locate/ybbrc

Identification and functional analysis of consensus androgen response elements in human prostate cancer cells☆

Kuniko Horie-Inoue[a], Hidemasa Bono[b], Yasushi Okazaki[b], Satoshi Inoue[a,c,*]

[a] *Division of Gene Regulation and Signal Transduction, Research Center for Genomic Medicine, Saitama Medical School, 1397-1 Yamane, Hidaka-shi, Saitama 350-1241, Japan*
[b] *Division of Functional Genomics and Systems Medicine, Research Center for Genomic Medicine, Saitama Medical School, 1397-1 Yamane, Hidaka-shi, Saitama 350-1241, Japan*
[c] *Department of Geriatric Medicine, Faculty of Medicine, The University of Tokyo, 7-3-1 Hongo, Bunkyo-ku, Tokyo 113-8655, Japan*

Received 26 October 2004
Available online 11 November 2004

Abstract

Androgen receptor (AR) recognizes and binds to 15-bp palindromic androgen response element (ARE) sequences with high affinity in vitro, which consist of two hexameric half-sites arranged as inverted repeats with a 3-bp spacer. Although a few near-consensus ARE sequences have been actually identified in the transcriptional regulatory regions of androgen-responsive genes, it has been unclear whether the exact consensus sequences function as bona fide AREs in vivo. A genome-wide in silico screening of palindromic AREs identified 563 exact consensus sequences in the human genome. The distribution of perfect palindromic AREs among the chromosomes is basically consistent with the length of chromosomes. Using human prostate cancer cell line LNCaP treated with a synthetic androgen R1881 as a model, in vivo AR binding abilities of 21 consensus AREs were analyzed by chromatin immunoprecipitation. Of 21 genomic fragments containing perfect AREs in chromosome X, 8 fragments recruited more ARs (>4-fold enrichment) even compared with the proximal ARE region of prostate-specific antigen. A couple of proximal genes or putative transcripts in the vicinity of the perfect AREs were found to be androgen-responsive analyzed by quantitative RT-PCR. Our results suggest that some of perfect palindromic AREs could function as in vivo AR binding sites in the human genome and regulate gene transcription.

Keywords: Androgen receptor; Androgen response element; Androgen-responsive gene; Chromatin immunoprecipitation; Prostate cancer

The androgen receptor (AR), a member of nuclear receptor superfamily that functions as a ligand-dependent transcription factor, plays an essential role in male sexual differentiation as well as prostate development and carcinogenesis. Forming complexes with coactivators and general transcription factors, ligand-stimulated AR binds to *cis*-acting androgen response elements (AREs) in the regulatory regions of androgen-responsive genes and modulates the transcription of target genes. The palindromic 15-bp sequence, which consists of two hexameric half-sites (5′-AGAACA-3′) arranged as an inverted repeat with a 3-bp spacer, has been identified as the consensus sequence for AR binding [1,2]. Although near-consensus ARE sequences that match at least 9 of 12 nucleotides have been found in the regulatory regions of several androgen-responsive genes [1], none of the perfect consensus ARE has yet been identified. A question arises whether the palindromic ARE consensus sequence functions as a bona fide AR binding

☆ *Abbreviations:* AR, androgen receptor; ARE, androgen response element; BCOR, BCL-6 interacting corepressor; ChIP, chromatin immunoprecipitation; GAPDH, glyceraldehyde-3-phosphate dehydrogenase; PCYT1B, phosphorylcholine transferase B; PSA, prostate-specific antigen; RT-PCR, reverse transcription-polymerase chain reaction.

* Corresponding author. Fax: +81 3 5800 6530.
E-mail address: INOUE-GER@h.u-tokyo.ac.jp (S. Inoue).

0006-291X/$ - see front matter © 2004 Elsevier Inc. All rights reserved.
doi:10.1016/j.bbrc.2004.10.174

site that regulates transcription of proximal androgen-responsive genes in vivo.

In the present study, we identified perfect ARE sites in silico based on the human genome sequences that are available from public database and analyzed experimentally the functions of consensus AREs in terms of AR binding abilities in vivo and potential androgen-dependent transcription regulation of proximal genes. Focusing on the chromosome X, we actually identified several AR binding sites among the computationally identified perfect ARE sequences. A couple of proximal RNA transcripts in the vicinity of perfect AREs were androgen-responsive, suggesting that some of the consensus ARE sites have potentials to activate transcription of nearby genes. Our combined approach of characterization of ARE sites will contribute to the systematic elucidation of the gene regulatory network mediated by androgen, which will be pivotal for the development of prostate cancer.

Materials and methods

Bioinformatics. Consensus AREs in the human genome (Human 34d Gene Build retrieved from Ensembl ftp site [3]) were screened utilizing in-house Perl script and a program for regular expression search of a nucleotide sequence (program name: dreg) in EMBOSS package [4]. The regular expression pattern for ARE was obtained from a recent literature by Nelson et al. [1], in which the palindromic 5′-AGAACAnnnTGTTCT-3′ sequence corresponding to the ARE sequence in TRANSFAC database [5] was used as a consensus sequence.

Cell culture. Human prostate cancer LNCaP cells were purchased from American Type Culture Collection (Rockville, MD) and maintained in RPMI 1640 supplemented with 4.5 g/dl glucose, 1 mM sodium pyruvate, 10 mM Hepes, and 10% fetal bovine serum (FBS). Prior to hormone addition, cells were cultured for 2 days in phenol red-free RPMI 1640 supplemented with 5% dextran–charcoal stripped FBS (dcc-FBS) and one day in phenol red-free RPMI 1640 supplemented with 2.5% dcc-FBS.

Chromatin immunoprecipitation assay. LNCaP cells (8×10^7) after 72-h hormone depletion were treated with 10 nM of R1881 (NEN Life Science Products, Boston, MA) or 0.1% ethanol for 24 h. Cells were fixed in 1% formaldehyde for 5 min at room temperature. Chromatin was sheared to an average size of 500 bp by sonication using a Bioruptor ultrasonicator (Cosmo-Bio, Tokyo, Japan). Lysates corresponding to 2×10^7 cells were rotated at 4 °C for overnight with 3 μg of polyclonal anti-AR antibody (H-280, Santa Cruz Biotechnology, Santa Cruz, CA) or non-specific rabbit IgG (Sigma). Salmon sperm DNA/protein A–agarose (Upstate Biotechnology, Lake Placid, NY) was added and incubated for 2 h. Washing and reversal of cross-links was performed as described [6]. Precipitated DNA fragments were quantified by quantitative real-time PCR using the Applied Biosystems 7000 sequence detector (Foster City, CA) based on SYBR Green I

Table 1
Primers for quantitative ChIP assay and RT-PCR

Target	Forward primer sequence	Reverse primer sequence
ARE sites[a]		
X1	5′-GTGCTTTGCAGGCAGTGATG-3′	5′-TCATTCCTTTGTTTTACTGAGAGTTCA-3′
X2	5′-GCAACTGCAAAGCCAAAATG-3′	5′-ATCTGTTTCCCATCTCCGTATATGTA-3′
X3	5′-CCAAAAAGCCCCTAGGAAAGA-3′	5′-AACCAGCAGTGTTTGCTCCAA-3′
X4	5′-CCAGGGCTCCTCCTTTGG-3′	5′-ATCTGACCCTGTGCATTTGAGA-3′
X5	5′-ACAGGTGCAAACACACAAAAGC-3′	5′-ACCCTTTCCTGGTCCTTTGTC-3′
X6	5′-ACAACAAATTCACCTGAGGTTCATAT-3′	5′-GCTTATCCAGGGACATCAGGTT-3′
X7	5′-CCAAATATGTCCATTCATCCAACA-3′	5′-GGAAACATACGCATTGCCTAGAA-3′
X8	5′-TTAATGTCTCTGTGAACCATTCTTCTG-3′	5′-GGTAACTACTGGGAAGGGAATTAGC-3′
X9	5′-CTGAGGGCGGACCTTGTTAAG-3′	5′-GCTCCAGGAGCTCTACGAGGTT-3′
X10	5′-TTAACAAAAAGCCAAGAGTGACAA-3′	5′-ACATCTTTTTTTCTTTGCTCCAGAA-3′
X11	5′-GAAGGTCCGTTGAGTTTATCTATTC-3′	5′-GGAAGTTTTCAGACATTTCTTCAG-3′
X12	5′-TGTGTAAAACACTCAACAAGTTAGAACA-3′	5′-CCTTGCCTTCTTTCTGATCTTAGG-3′
X13	5′-CGGGCAGTGGAAAAGCAA-3′	5′-CCTGTGTCTCCTCAAAAGAAATGA-3′
X14	5′-CAGTTCTGATGTGGTAAGTGGAAGA-3′	5′-GGTGAGTGGCGAAGTGGTAAC-3′
X15	5′-TCCCAGTTTCTCAGGGATCACT-3′	5′-TCTCCCACATGAAACAACTAAAAAGT-3′
X16	5′-AGGGCCAGCTTTATTAAGAACAGA-3′	5′-CTGTAGGAGCCCTGCAAGGT-3′
X17	5′-AATGTTTGCTTACTGCAAGTGTACT-3′	5′-GTGTGGGTTGCATGTACTGC-3′
X18	5′-TTTTGTCCCAGTCCTACATCTTGTT-3′	5′-GCTCATGTCCTCTATAGCCCTACA-3′
X19	5′-GCAGATTTTAAACCACAGTATTAAGTCAAA-3′	5′-GAGGGTACAGAGGAGCCAAAGA-3′
X20	5′-CAGAATCTGTAGCCAAACTACGAACT-3′	5′-CAGCCTGGCCCTTTTACTGA-3′
X21	5′-TCCTAGGAGAAATGGCTGATTCC-3′	5′-CAAAGTGTCATTATTCAGTGTACAACTCTAC-3′
PSA proximal promoter	5′-TCTGCCTTTGTCCCCTAGAT-3′	5′-AACCTTCATTCCCCAGGACT-3′
PSA distal promoter	5′-ACAGACCTACTCTGGAGGAAC-3′	5′-AAGACAGCAACACCTTTTT-3′
PSA coding	5′-GCCCTGCCCGAAAGG-3′	5′-GATCCACTTCCGGTAATGCA-3′
GAPDH coding[b]	5′-GGTGGTCTCCTCTGACTTCAACA-3′	5′-GTGGTCGTTGAGGGCAATG-3′
PCYT1B coding	5′-GCAGGGATGTTCGTTCCAA-3′	5′-CTGGTAATGATGTCCGATGTTGA-3′
NM_144657 coding	5′-CAGCAACAACAGGAACCTCTTTG-3′	5′-CGAGCAATATTAACCACATTTCTGA-3′
Genscan00000043157[c]	5′-GACAGTAGACTTCCCAGAGCACATAG-3′	5′-TCTCCTGTTTCAGTCCAATTCTGA-3′

[a] The position of ARE sites are described in Table 2.
[b] Primers for GAPDH coding were used for both ChIP assay and RT-PCR.
[c] Genscan00000043157: a putative transcript predicted by the Ensembl pipeline analysis system using the Genscan prediction program.

fluorescence. Primer pairs were designed by Primer Express ver. 2.0 software (Applied Biosystems), generating perfect ARE-containing fragments with the requirements of primer T_m temperature at basically 58–60 °C and the requirements of amplicon length for 50–150 bp. The protocol of PCR was 2 min at 50 °C, 10 min at 95 °C, and 40 cycles of 15 s at 95 °C and 1 min at 60 °C. To determine relative differences among the treatment groups for the chromatin immunoprecipitation (ChIP) assays we used the $\Delta\Delta C_t$ method as outlined in the Applied Biosystems protocol for reverse transcriptase-PCR. The average threshold cycle (C_t) for the duplicate was used in all subsequent calculations. A genomic fragment corresponding to GAPDH was used as an external standard. Genomic fragments containing proximal or distal ARE in the promoter region of prostate-specific antigen (PSA) (−250 to −39 bp and −4170 to −3978 bp from the transcriptional initiation site, respectively) [6] were used as positive controls. The sequences of the primers used in ChIP assays (synthesized by Sigma Genosys, Japan) are described in Table 1.

Quantitative reverse transcription-PCR. Total RNA was extracted from R1881-treated or 0.1% ethanol-treated LNCaP cells for 24 h using ISOGEN reagent (Nippon Gene, Tokyo, Japan). First strand cDNA was generated from RNase-free DNase I-treated total RNA by using SuperScript II Reverse Transcriptase (Invitrogen, Carlsbad, CA) and pdT_{12-18} primer (Amersham Biosciences, Piscataway, NJ). Proximal genes or putative transcripts that locate within a ±20-kb distance from perfect AREs were selected for reverse transcription-PCR (RT-PCR) analysis. cDNAs were quantified by quantitative real-time PCR using the Applied Biosystems 7000 sequence detector based on SYBR Green I fluorescence as described above. The primer sequences for the amplifications are described in Table 1.

Results

In silico identification of perfect palindromic ARE sequences in the human genome

In terms of palindromic ARE sequences composed of two AGAACA sequences separated by a 3-bp spacer, a few near-consensus sequences, but no perfect palindromic sequences have been identified among human androgen-responsive genes. In order to answer the question whether perfect palindromic ARE sequences do function as in vivo AR binding sites, we computationally searched all the consensus ARE sequences in the human genome utilizing in-house Perl script and a program for regular expression pattern search of a nucleotide sequence in EMBOSS package (program name: dreg) [4]. The screening defined 563 elements, noting that the number of sites was larger than the expected frequency in random DNA sequences as calculated by the total number of base pairs in the genome divided by the frequency of a sequence with specified base pairs at 12 positions ($3{,}223{,}443{,}491/4^{12} = 192$). The distribution of consensus sequences among the chromosomes is generally consistent with chromosomal size, the average frequency of ARE being 17.3 ± 4.3 sites per 100 Mb (Figs. 1A and B).

In vivo AR recruitment of perfect AREs on chromosome X

To investigate whether the computationally identified ARE sequences with perfect motifs recruit AR in vivo, we performed ChIP assay in AR-positive LNCaP cells. The chromosome X was selected as an experimental model, in which AR gene itself locates. The distribution of 21 perfect ARE sites on chromosome X is mapped in Fig. 2 and the detailed information of ARE (X1–X21) sites including nucleotide positions and sequences is in Table 2. None of the consensus AREs clustered in chromosome X within 50 kb, as the narrowest distance between X5 and X6 was 57.7 kb.

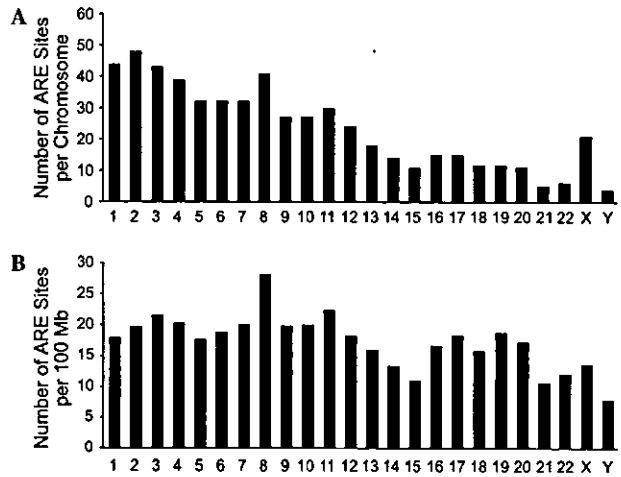

Fig. 1. Distribution of perfect palindromic AREs in the human genome. (A) The number of perfect consensus AREs found per chromosome. (B) The ratio between the number of perfect AREs and the length of chromosome (sites per 100 Mb).

We performed quantitative PCR using genomic DNAs from LNCaP cells with 24-h treatment of R1881 (10 nM) or 0.1% ethanol, immunoprecipitated by either a specific AR antibody or non-specific rabbit IgG (Fig. 3). The AR association with proximal and distal promoter regions of PSA including ARE sequences was more than 3.5-fold and 60-fold increased by R1881 treatment, respectively. Of 21 genomic fragments containing perfect AREs in chromosome X, 8 fragments recruited more ARs (>4-fold enrichment) compared with the proximal ARE region of PSA. No particular specificity of 3-bp spacer sequences for AR recruitment has been found; for example, both ARE X5 and X6 sites contain a GCC spacer while fold enrichment of AR recruitment was 1.2-fold and 7.2-fold, respectively. In the case of X17 and X19 sites possessing an identical GCA spacer, fold difference of AR binding was 9.5-fold and 2.0-fold, respectively.

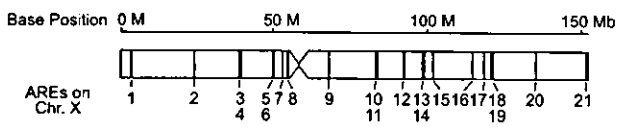

Fig. 2. Positions of the perfect palindromic AREs on chromosome X. Indicated numbers 1–21 correspond to perfect ARE sites.

Table 2
Proximal RNA transcripts in the vicinity of perfect palindromic AREs in chromosome X

AREID[a]	Start	Stop	ARE sequence	Proximal transcript	Ensembl ID No.	Location of ARE site[b]
X1	3181583	3181597	AGAACAtggTGTTCT	PRKX	ENSG00000183943	Within
X2	23945954	23945968	AGAACActaTGTTCT	PCYT1B	ENSG00000102230	Within
X3	38720672	38720686	AGAACAaagTGTTCT	*Ab-initio* Genscan transcript[c]	GENSCAN00000046001	Within
X4	38970910	38970924	AGAACAaagTGTTCT	BCOR	ENSG00000183337	5′ (3 kb)/within[d]
X5	49168004	49168018	AGAACAgccTGTTCT	*Ab-initio* Genscan transcript	GENSCAN00000107032	3′ (8 kb)
X6	49225713	49225727	AGAACAgccTGTTCT	*Ab-initio* Genscan transcript	GENSCAN00000043157	3′ (10 kb)
X7	52321185	52321199	AGAACAttaTGTTCT	O60275	ENSG00000124313	5′ (4 kp)
X8	53952953	53952967	AGAACAtaaTGTTCT	PFKFB1	ENSG00000158571	Within
X9	67507044	67507058	AGAACAgaaTGTTCT	*Ab-initio* Genscan transcript	GENSCAN00000115882	Within
X10	82472510	82472524	AGAACAatgTGTTCT	NM_144657	ENSG00000165259	Within
X11	83327890	83327904	AGAACAttcTGTTCT	NM_024921	ENSG00000124429	Within
X12	91506977	91506991	AGAACAaaaTGTTCT	*Ab-initio* Genscan transcript	GENSCAN00000029252	Within
X13	98772894	98772908	AGAACAagaTGTTCT	SYTL4	ENSG00000102362	5′ (5 kb)
X14	98951387	98951401	AGAACAtctTGTTCT	Ensembl novel transcript	ENST00000328526	Within
X15	101412450	101412464	AGAACAgctTGTTCT	NGFRAP1	ENSG00000166681	3′ (8 kb)
X16	114061336	114061350	AGAACAgaaTGTTCT	*Ab-initio* Genscan transcript	GENSCAN00000064921	Within
X17	118442517	118442531	AGAACAgcaTGTTCT	CUL4B	ENSG00000158290	Within
X18	120798222	120798236	AGAACActaTGTTCT	*Ab-initio* Genscan transcript	GENSCAN00000054945	Within
X19	121144935	121144949	AGAACAgcaTGTTCT	GRIA3	ENSG00000125675	Within
X20	134752049	134752063	AGAACAactTGTTCT	Q96NB7	ENSG00000173971	Within
X21	151348988	151349002	AGAACAcccTGTTCT	NM_152274	ENSG00000147382	5′ (16 kb)

[a] ARE ID X1–X21 correspond to the numbers 1–21 in Fig. 2.
[b] Location of ARE site indicates the proximity to annotated genes or putative transcripts.
[c] *Ab-initio* Genscan transcript: putative transcript predicted by the Ensembl pipeline analysis system using the Genscan prediction program [7].
[d] BCOR has two different initiation sites.

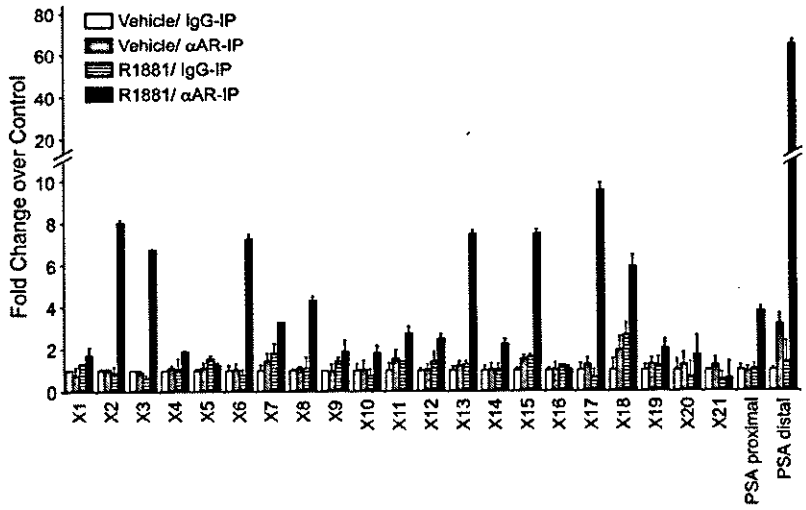

Fig. 3. Chromatin immunoprecipitation assay in LNCaP cells. Cells after 72-h hormone depletion were treated with 10 nM R1881 or 0.1% ethanol as a vehicle for 24 h. Quantitative PCR was performed using ChIP DNA samples immunoprecipitated by rabbit polyclonal anti-AR antibody (αAR-IP) or non-specific rabbit IgG (IgG-IP). In each case, fold enrichment values in R1881-treated samples immunoprecipitated by anti-AR antibody and non-specific rabbit IgG (R1881/αAR-IP and R1881/IgG-IP) as well as vehicle-treated ones precipitated by anti-AR antibody (vehicle/αAR-IP) were compared with those in vehicle-treated samples precipitated by non-specific rabbit IgG (vehicle/IgG-IP). Each result is the mean ± SEM of two independent experiments in duplication (four determinants). Prostate-specific antigen (PSA) proximal and distal promoter regions are served as positive controls.

Potential transcriptional regulation of proximal genes in the vicinity of perfect AREs

To examine whether perfect AREs regulate transcriptional activities of proximal genes, we next performed quantitative RT-PCR for RNA transcripts in the vicinity of consensus ARE sites. Proximal genes were selected for each ARE site based on the following requirements of ARE location: (1) within an annotated gene, (2) within 20-kb upstream to 5′ end of a known gene, or (3)

within 20-kb downstream to 3′ terminus of a known gene (Table 2). If no annotated genes exist in the vicinity of ARE sites, putative transcripts predicted by the Ensembl pipeline analysis system using the Genscan prediction program [7] and mapped on the Ensembl genome browser were chosen (i.e., *ab-initio* Genscan transcripts). Ten out of 21 AREs are located within introns of known genes or a novel transcript, 4 sites in the 5′ regions of annotated genes [ARE X4 is counted in both 5′ region and within intron 1 of BCOR (BCL-6 interacting corepressor) due to variants], one site in the 3′ regions of a known gene. No known genes were found in the vicinity of seven ARE sites.

Quantitative RT-PCR was conducted using the first-strand cDNAs derived from LNCaP cells treated with a synthetic androgen R1881 or 0.1% ethanol as a vehicle for 24 h. Two annotated genes and one putative transcript exhibited significant increase in transcript expression levels agonist-dependently (Fig. 4). PCYT1B (phosphorylcholine transferase B) is a gene encoding an enzyme that controls phosphatidylcholine synthesis [8,9]. PCYT1B may be related to the reproduction function as it is highly expressed in testis, placenta, and ovary. Perfect ARE (X2) locates within intron 7 of PCYT1B. In regard to NM_144657, the gene encodes 690 amino acids and contains perfect ARE (X10) within intron 3. Although the fold enrichment of R1881-activated AR binding in ARE X10 was smaller than that in the PSA proximal promoter region, yet it is statistically significant ($P < 0.05$). The gene NM_144657 is found to possess two HOX homeobox domains by analyzing domain architectures using a Simple Modular Architecture Research Tool (SMART) on InterPro databases (http://www.ebi.ac.uk/interpro/databases.html). The gene may be a nuclear DNA-binding protein that is involved in the transcriptional regulation of developmental processes. Concerning an *ab-initio* Genscan transcript (ID: Genscan00000043157) that is located 10-kb upstream to consensus ARE (X6), the sequence does not exhibit overall similarity with any characterized human gene.

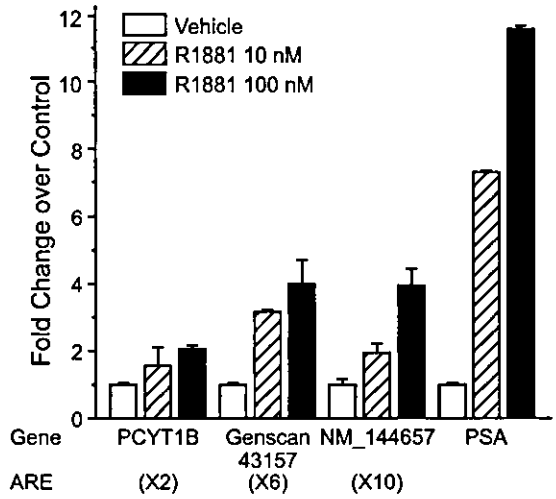

Fig. 4. Quantitative RT-PCR of proximal genes in the vicinity of perfect AREs. LNCaP cells after 72-h hormone depletion were treated with R1881 (10 or 100 nM) or 0.1% ethanol as a vehicle for 24 h. Real-time PCR was conducted using the first strand cDNAs generated from the total RNAs of the cells. PCYT1B, Genscan43157 (Genscan00000043157), and NM_144657 are located in the vicinity of ARE X2, X6, and X10, respectively. Each result is the mean ± SEM of two independent experiments in duplication (four determinants). PSA is served as a positive control.

Discussion

In the present study, we identified 563 perfect palindromic ARE sequences in the human genome, whose frequency of occurrence is more than our initial expectation of approximately 200 sites. We functionally analyzed 21 consensus AREs on chromosome X as a sample of the population. Eight of 21 AREs recruited more ARs (>4-fold enrichment) upon ligand treatment even compared with the proximal ARE region of PSA, as determined by ChIP assay using human prostate cancer LNCaP cells. It was also shown that distal ARE region of PSA showed by far the highest recruitment of AR. In regard to the expression of transcripts that locate with ±20 kb from perfect AREs, two annotated genes and one putative transcript were upregulated ligand-dependently, suggesting that these proximal genes are potentially androgen-responsive genes.

Our results reveal two interesting points in the field of steroid receptors. One is the frequency of occurrence of hormone response elements. Based on our data of ChIP assay along chromosome X, there might be at least 200 perfect ARE sequences that actually function as AR binding sites in the entire human genome. A recent computational analysis of near-consensus estrogen response elements, in which 10 specified nucleotides and 2 nucleotide choices at 2 positions out of 12 bp, revealed that there are approximately 70,000 sequences in the human and mouse genomes [10]. By the experimental approach of tiling array of chromosomes 21 and 22 hybridized with immunoprecipitated DNAs, there might be large number of transcription factor binding sites with a minimal estimate of 12,000 for Sp1, 25,000 for c-Myc, and 1600 for p53 [11]. Taking together our present results and the estimation of transcription factors by others, there may be at least several thousand sites of functional AREs in the human genome.

The second interesting point is the relationship of perfect AREs to proximal genes and potential transcription regulation by consensus AREs. In our results, nearly half of the perfect AREs (10 of 21) on chromosome X are located within introns of annotated genes